Studies of Integrable One-Dimensional Quantum Systems

Nathan Keenan B.Sc.

This thesis is presented for the degree of Masters by Research
to the University of Maynooth,
Department of Theoretical Physics.

June 2021

Department Head:
Prof. Peter Coles

Research Advisor:
Dr. Masudul Haque

Contents

Abstract

In this thesis, I use the Bethe Ansatz (BA) to study various one-dimensional models. I first go through some background on the BA (both the coordinate and algebraic forms). I start the study by using the BA to compare bound state occurrences between the 2-particle XXZ, Bose–Hubbard, and Fermi–Hubbard models. In the next chapter, I introduce 'quenches' and use the BA in order to calculate quench overlaps in the Lieb–Liniger model. In the final chapter, I introduce the spatial von Neumann bipartite entanglement entropy and use the BA in order to calculate this entropy in the Lieb–Liniger model.

Chapter 1

Introduction

1.1 Overview

One-dimensional systems have long proven to be an important tool in physics, by providing a manageable environment (computationally and conceptually) to study complex physical phenomena. The Heisenberg spin chain is a convenient environment in which to study quantum magnetism, and has even been realised in experimental environments [1, 2]. The Bose and Fermi Hubbard models are the simplest models for studying bosons and fermions respectively on a lattice [3, 4, 5]. The Lieb–Liniger model offers a simple picture of interacting bosons in the continuum, with the interaction being only on contact. An example of a system well described by the Lieb–Liniger model is the well–known Bose–Einstein condensate whose existence was first predicted theoretically by Einstein in the 1920s [6] and has been the centre of a lot of study since.

All of these models have something in common: they are all integrable systems. In this context, an integrable system is one that is solvable by a mathematical technique [7] known as the Bethe ansatz. In other words, the energy eigenstates of these models can all be exactly and analytically calculated via this technique. Systems that are not integrable are known as chaotic systems, and an exact form of the eigenstates of these systems does not in general exist. There isn't an easy way of seeing *a priori* whether or not

a model is integrable, but a good indicator of this solvability is if the model has many integrals of motion (referred to as conserved charges in this case) that preserve locality [8]. We will see more of a discussion of these charges in section (1.3.3) and section (3.2).

With the lattice models (XXZ, Bose–Hubbard, Fermi–Hubbard), I am interested in the bound state occurrence probabilities in eigenstates. I analyse the two-particle systems for each model by plotting the 'bound state probabilities' for systems of varying size, and I use the Bethe ansatz to explain the most obvious patterns in this data. I find that most of the interesting results are easy to analytically verify in the momentum language of the system, but the Bethe ansatz offers a more natural setting to study the systems in with rapidities, and I explore this language to obtain more results. I find that there are subtle differences between the bound state dependence on the anisotropy of the XXZ chain, and the bound state dependence on the interaction energy of the BH model. I also show that the bound state dependency in the 2-particle Fermi–Hubbard on the interaction energy is essentially the same as that in the 2-particle Bose–Hubbard, despite the corresponding Hilbert spaces for the two models being different.

With the Lieb–Liniger model, I investigate what is called 'quench overlaps'. I motivate these calculations by introducing the idea of a 'quench' [9]. In order to come up with a way to study how a random state evolves under the Lieb–Liniger Hamiltonian, we need a way of simulating a 'random' state. This is done by picking a value of the interaction parameter of the system (usually 0), and then watching how eigenstates of that system evolve when you suddenly change the interaction parameter. This instantaneous change is known as a 'quench'. Expanding these eigenstates in terms of the eigen-basis of the new system gives us these 'quench overlaps'. In particular, I focus on the overlaps with parity symmetric states. These are states that are symmetric under parity reflection. They are of interest as they have an important interplay with what are known as the conserved charges [10] of the system.

Lastly, I look at the spatial von Neumann bipartite entanglement entropy [11, 12] of the Lieb Liniger model with periodic boundary conditions. I first

elaborate on what I am actually calculating, and then I offer a simple expression that allows this entropy to be calculated analytically for every particle sector (although the computation of this expression is still of exponential computational complexity). The method used does not use any special features of the Lieb–Linger model and so it should follow easily for any integrable model on S^1. Numerical methods to calculate this entropy exist [12] (also, it is known that entanglement entropy can easily be extracted from DMRG simulations, and such simulations are possible for the Lieb–Liniger model, see [13]) but to the best of my knowledge this is the first time a method for an analytic calculation is presented.

1.2 The Coordinate Bethe Ansatz

The Bethe ansatz as a technique for solving one-dimensional quantum Hamiltonians, originated from the work of Hans Bethe in 1931[14], in the form of a method to find exact expressions for the eigenfunctions of the periodic isotropic spin-1/2 Heisenberg chain:

$$H = -J \sum_{n=1}^{L} \boldsymbol{S_n} \cdot \boldsymbol{S_{n+1}}, \tag{1.1}$$

where J is the constant spin coupling at each site, $\boldsymbol{S}_n$ is the spin operator at site n, and the periodic boundary conditions are equivalent to identifying site $L+1$ with site 1. This technique was later generalized in order to solve certain one-dimensional systems (known as integrable systems), in what is now known as the coordinate Bethe ansatz. This technique consists of using what is known as a Bethe substitution [15] in order to determine the spectrum of the system. I will use the XXZ model - a slight alteration on Bethe's original target for his ansatz - in order to demonstrate this technique.

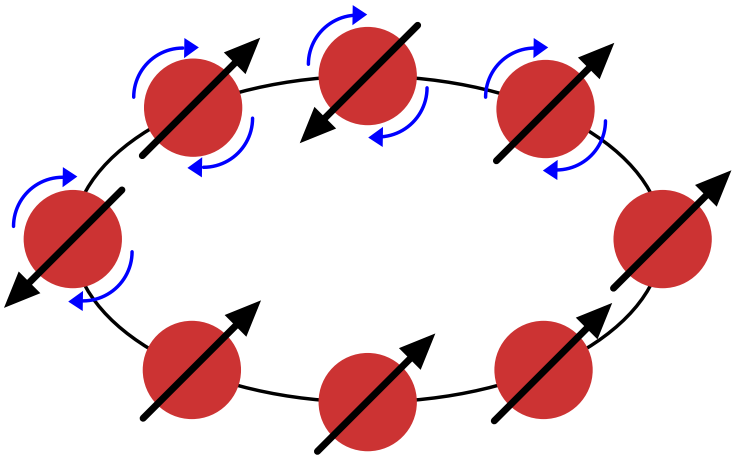

Figure 1.1: Schematic representing the Heisenberg chain. The rotating arrows indicate possible pairs of particles that will flip spin at the shown instant.

1.2.1 Solving the XXZ model with the Coordinate Bethe Ansatz

The XXZ model is similar to that in equation (1.1), except we introduce spin-anisotropy via the spin along the z-axis:

$$H_\Delta = -J \sum_{n=1}^{L} \left[S_n^x S_{n+1}^x + S_n^y S_{n+1}^y + \Delta S_n^z S_{n+1}^z \right]. \tag{1.2}$$

Even after introducing a new parameter Δ to the Hamiltonian, the system turns out to still be integrable (ie, solvable by the Bethe ansatz), and we retrieve the isotropic Heisenberg chain by setting $\Delta = 1$. Noting that the total z-spin projection $S^z = \sum_n S_n^z$ commutes with the Hamiltonian, the energy eigenstates can be analysed in separate total S^z sectors. With this in

mind, we can rewrite the Hamiltonian using spin flip operators $S_n^{\pm} = S_n^x \pm i S_n^y$:

$$H_\Delta = -J \sum_{n=1}^{L} \left[\frac{1}{2} \left(S_n^+ S_{n+1}^- + S_n^- S_{n+1}^+ \right) + \Delta S_n^z S_{n+1}^z \right]. \tag{1.3}$$

We can then arrange the eigenstates into sectors with a given number d of downspins with respect to the ferromagnetic state $|F\rangle$ with $S^z = L/2$.

The $d = 0$ sector consists only of the ferromagnetic state $|F\rangle$, and has energy density $E_0/L = -J\Delta/4$.

The $d = 1$ subspace is spanned by the L vectors $|n\rangle = S_n^- |F\rangle$, $n = 1, ..., L$. The main idea surrounding the Bethe ansatz is to use the translational invariance of this model to make the 'ansatz' that if $|\psi\rangle$ is an eigenstate of H_Δ, then it can be written as a translationally invariant superposition of plane waves:

$$|\psi_k\rangle = \frac{1}{\sqrt{L}} \sum_{n=1}^{L} e^{ikn} |n\rangle . \tag{1.4}$$

It turns out that this is indeed an eigenstate of H_Δ, with energy density $(E - E_0)/L = J(\Delta - \cos(k))$. Implementing boundary conditions allows us to find allowed values for k. Continuing with periodic boundary conditions, we get that $k = \frac{2\pi I}{L}$, $I = 0, 1, ..., L-1$. We call I a Bethe quantum number. These numbers help characterise the Bethe states of our system.

We can continue this analysis in the $d = 2$ sector, except we have to be wary of symmetry requirements involved in swapping downspins. We look for eigenstates of the form:

$$|\psi_{k_1,k_2}\rangle = \sum_{1 \le n_1 < n_2 \le L} |n_1, n_2\rangle \left(A_{12} e^{i(k_1 n_1 + k_2 n_2)} + A_{21} e^{i(k_2 n_1 + k_1 n_2)} \right). \tag{1.5}$$

Plugging this state into the Hamiltonian and requiring that it is an eigenstate gives us an expression for the relative amplitude A_{12}/A_{21}. It is easily checked that this ratio has unit magnitude, so we introduce a scattering phase θ_{12}:

$$A_{12}/A_{21} = e^{i\theta_{12}} = -\frac{e^{i(k_1+k_2)} + 1 - 2\Delta e^{ik_1}}{e^{i(k_1+k_2)} + 1 - 2\Delta e^{ik_2}}. \tag{1.6}$$

We can then write a general unnormalized eigenstate in this sector as:

$$|\psi_{k_1,k_2}\rangle = \sum_{1\leq n_1<n_2\leq L} |n_1,n_2\rangle \left(e^{i(k_1n_1+k_2n_2+\frac{1}{2}\theta_{12})} + e^{i(k_2n_1+k_1n_2+\frac{1}{2}\theta_{21})}\right), \quad (1.7)$$

where $\theta_{21} = -\theta_{12}$.

We use periodic conditions again to find allowed values of the parameters k_1, k_2, which we will refer to as the momenta of the state from now on:

$$Lk_{1,2} = 2\pi I_{1,2} \pm \theta_{12}, \quad (1.8)$$

where $I_1, I_2 = 0, 1, ..., L-1$ are the Bethe quantum numbers characterising the state.

We then move onto the $d > 2$ downspin sector. This sector is where the Bethe ansatz becomes non-trivial, and we must work to break all interactions up into a sum of two-particle interactions in order to be able to use the Bethe ansatz. Thankfully, in the case of the XXZ model, this sector is handled similarly to the $d = 2$ sector, except the permutation sum in equation (1.5) is carried out over the entirety of the symmetric group S_d. If Q is the standard ordering of the particles $(1, 2, ..., d)$, then:

$$\left|\psi_{\vec{k}}\right\rangle = \sum_{1\leq n_1<...<n_d\leq L} |n_1,...,n_d\rangle \sum_{\sigma\in S_d} A_{\sigma Q} \exp\left(i\sum_{j=1}^{d} k_{\sigma_j} n_j\right). \quad (1.9)$$

For ease of notation, I will drop the Q in the subscripts of the amplitudes. Given two permutations σ and τ such that we get σQ by swapping indices i and j in τQ where $\sigma_i < \sigma_j$, we have:

$$\frac{A_\sigma}{A_\tau} = e^{i\theta_{\sigma_i,\sigma_j}}. \quad (1.10)$$

Then we can build any A_σ, up from A_{id}:

$$\frac{A_\sigma}{A_{\text{id}}} = \prod_{i<j} e^{i\theta_{\sigma_i,\sigma_j}} = (-1)^\sigma \prod_{i<j} \frac{e^{i(k_{\sigma_i}+k_{\sigma_j})} + 1 - 2\Delta e^{ik_{\sigma_i}}}{e^{i(k_{\sigma_i}+k_{\sigma_j})} + 1 - 2\Delta e^{ik_{\sigma_j}}}, \quad (1.11)$$

and so we can write:

$$\left|\psi_{\vec{k}}\right\rangle = \sum_{1\leq n_1<\ldots<n_d\leq L} |n_1,...,n_d\rangle \sum_{\sigma\in S_d} \exp\left(i\sum_{i=1}^{d} k_{\sigma_j} n_j + \frac{i}{2}\sum_{i<j}\theta_{\sigma_i\sigma_j}\right). \quad (1.12)$$

As before, we use periodic conditions to find the allowed values for k_j:

$$Lk_j = 2\pi I_j + \sum_{i<j}\theta_{ij}, \quad (1.13)$$

where again, $I_j = 0, 1, ..., L-1$ are the Bethe quantum numbers. The equations (1.13) are known as the Bethe equations for this system. They are generally nonlinear equations and thus quite hard to solve, but nevertheless allow us to write down exact expressions for the eigenstates and eigenenergies of our system.

1.2.2 Solving the 2-Particle Hubbard Models with the Coordinate Bethe Ansatz

Further discussions and details about calculations for the Hubbard models can be found at [16] and [4]. Let us start by introducing the Hamiltonian for the Bose–Hubbard model:

$$H_{BH} = \sum_{0\leq i\leq L}\left(b_i^\dagger b_{i+1} + b_i b_{i+1}^\dagger\right) + \frac{U}{2}\sum_{i=1}^{L} n_i(n_i-1), \quad (1.14)$$

where the $b_i^\dagger$ and b_i are the boson creation and annihilation operators at the i-th lattice site, and $n_i = b_i^\dagger b_i$ is the number operator at site i. The interaction energy U introduces an 'energy cost' for having two or more bosons on the same site. We again use periodic boundary conditions, by associating site $L+1$ with site 1.

The Hamiltonian for the Fermi–Hubbard model is given by:

$$H_{FH} = \sum_{\sigma\in\{\uparrow\downarrow\}}\sum_{0\leq i\leq L}\left(c_{i,\sigma}^\dagger c_{i+1,\sigma} + c_{i,\sigma} c_{i+1,\sigma}^\dagger\right) + \frac{U}{2}\sum_{i=1}^{L} n_{i\uparrow} n_{i\downarrow}, \quad (1.15)$$

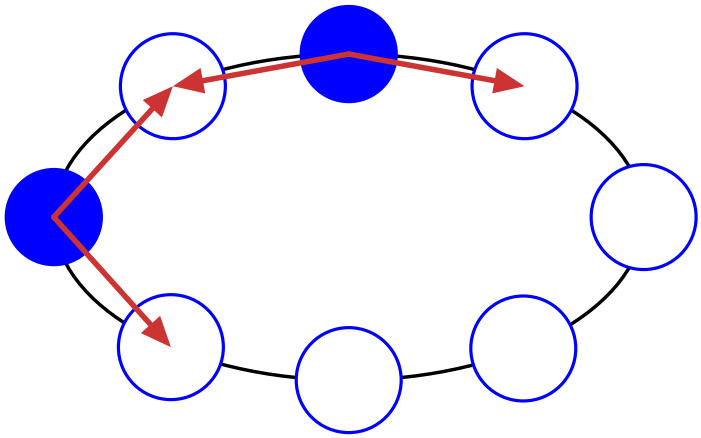

Figure 1.2: Schematic representing the periodic Bose–Hubbard chain. The arrows indicate where the particles are allowed to jump to next.

where the $c^\dagger_{i,\sigma}$ and $c_{i,\sigma}$ are the fermion creation and annihilation operators of spin σ at the i-th lattice site, and the $n_{i,\sigma} = c^\dagger_{i,\sigma} c_{i,\sigma}$ is the relevant number operator. An extra factor of $1/2$ is introduced on the interaction term in order to make the comparison to the Bose–Hubbard system equation 1.14) easier in section (2.3). It will be shown in section (2.4) that the features of the Fermi–Hubbard model (with periodic boundary conditions) that I am interested in can be explained by my analysis of the Bose–Hubbard model. Therefore in the rest of this section, I will only focus on the Bose–Hubbard model.

In order to find the energy eigenstates of this system, I proceed similarly to the previous section, skipping right to the ansatz for the general N particle sector.

I begin by making the same ansatz for the form of the Bethe wavefunction

as in equation (1.9) except now I will allow multiple occupancy of sites:

$$\left|\psi_{\vec{k}}\right\rangle = \sum_{1\leq n_1\leq\ldots\leq n_N\leq L} |n_1,...,n_N\rangle \sum_{\sigma\in S_N} A_\sigma \exp\left(i\sum_{j=1}^{N} k_{\sigma_j} n_j\right). \tag{1.16}$$

It turns out that this ansatz is only valid for $N \leq 2$ as the Bose–Hubbard model with arbitrary interaction energy U is not solvable by the Bethe Ansatz for $N \geq 3$ [17]. In short, this has to do with the fact that the Bethe ansatz works by turning every interaction into a collection of two particle interactions. This cannot be done when three or more bosons are on a single site.

Checking the consistency of this wavefunction with the eigenstate requirement of the Hamiltonian given by equation (1.14) for $N = 2$, we get a similar expression as in the XXZ case (1.6) for the amplitudes A_σ. The relevant phase factor between two permutations of the particles is given by [18]:

$$e^{i\theta} = \frac{\sin(k_1) - \sin(k_2) - iU/2}{\sin(k_1) - \sin(k_2) + iU/2}. \tag{1.17}$$

An interesting note is that the Fermi–Hubbard model is in fact solvable by the Bethe Ansatz for $N \geq 3$, but requires some extra technology known as the 'Nested Bethe Ansatz' [19].

1.2.3 Lieb–Liniger: The Coordinate Bethe Ansatz in the Continuum Limit

In this section, I will demonstrate how the coordinate Bethe ansatz can be used not only to determine the spectrum for spins and particles on a lattice, but also for particles in the continuum. For this, I will look at N bosons on the real line interacting via a δ-potential (The Lieb–Liniger model). The Hamiltonian takes the form:

$$H_c = -\sum_{j=1}^{N} \frac{\partial^2}{\partial x_j^2} + 2c\sum_{j<l} \delta(x_j - x_l). \tag{1.18}$$

We are interested in the case when the system is of a finite length L, with periodic boundary conditions.

For $c = 0$ we have a system of free bosons, $c > 0$ we have bosons that repel each other, and $c < 0$ we have bosons that attract each other.

To get an idea of how Bethe substitution [20] can be used to solve this system, we begin by looking at the 2-particle case:

$$H_c = -\frac{\partial}{\partial x_1^2} - \frac{\partial}{\partial x_2^2} + 2c\delta(x_1 - x_2). \tag{1.19}$$

We take advantage of bosonic symmetry to write a candidate eigenfunction $\psi(x_1, x_2)$:

$$\psi(x_1, x_2) = f(x_1, x_2)\theta(x_1 - x_2) + f(x_2, x_1)\theta(x_2 - x_1), \tag{1.20}$$

where $\theta(x)$ is the Heaviside step function. Similar to the case on a lattice, we look for solutions in the form of a superposition of plane waves:

$$f(x_1, x_2) = A_{12}e^{i(k_1x_1+k_2x_2)} + A_{21}e^{i(k_2x_1+k_1x_2)}. \tag{1.21}$$

Solving the eigenvalue equation [20], we get:

$$\frac{A_{12}}{A_{21}} = e^{i\theta(k_1-k_2)} \ , \ \theta(k) = \pi - 2\arctan\left(\frac{k}{c}\right). \tag{1.22}$$

We make the jump to the N particle case similarly to before; with full symmetrization of the wavefunction of the plane waves over x and k:

$$\psi(\vec{x}; Q) = \sum_{\sigma \in S_N} A_{\sigma Q} \exp\left(i \sum_{j=1}^{N} k_{\sigma_j} x_j\right), \tag{1.23}$$

where Q is the particle ordering, corresponding to some simplex in $\mathbb{R}$. For this model, it is useful to introduce the domain $\mathbf{1} = \{\vec{x} \in \mathbb{R} | 0 \leq x_1 < x_2 < ... < x_N \leq L\}$. Note that if we know the wavefunction in one simplex, by symmetry we know it everywhere. We will thus drop the Q dependence when discussing a chosen 'standard' simplex, say, $\mathbf{1}$.

Following along similar lines to the last section, if two permutations σ and τ differ by one transposition of indices, we have the two particle scattering phase:

$$\frac{A_\sigma}{A_\tau} = e^{i\theta(k-k')} = \frac{k-k'+ic}{k-k'-ic} = -2\arctan\frac{k}{c} + \pi, \tag{1.24}$$

where k and k' are the relevant momenta being interchanged. Like before, we can then build up an arbitrary amplitude A_σ from A_{id} up to normalization of $\psi(\vec{x})$:

$$A_\sigma = (-1)^\sigma \prod_{j<l}(k_{\sigma_j} - k_{\sigma_l} + ic). \tag{1.25}$$

To find the allowed values for $\vec{k}$, we must solve the Bethe equations. These again come from the boundary conditions for the system. As before, we are interested in periodic boundary conditions. We require that:

$$\psi(x_1, x_2, ..., x_j + L, ..., x_N) = \psi(x_1, x_2, ..., x_j, ..., x_N). \tag{1.26}$$

To get the left hand side above, we must scatter particle j through every other particle to get back to its starting position, and so it picks up a phase equal to the sum of the phases associated to each scattering event. We also pick up a dynamic phase of e^{ik_jL} from travelling around a circle of length L. This gives us the following equation:

$$A_\sigma = A_{\sigma R} e^{ik_{\sigma_j}L}, \tag{1.27}$$

where $R\{j, j+1, ..., N, 1, 2, ..., j-1\} = \{j+1, ..., N, 1, 2, ..., j-1, j\}$. This in combination with equation (1.25) gives us the Bethe equations for this system:

$$e^{ik_jL} = \prod_{l\neq j}\left(\frac{k_j - k_l + ic}{k_j - k_l - ic}\right). \tag{1.28}$$

1.3 The Algebraic Bethe Ansatz

In this section I will introduce a more modern adaptation of the Bethe Ansatz; The Algebraic Bethe Ansatz (ABA) [8, 20, 21]. The main use of

the ABA is that systems that are solvable by the Bethe ansatz have a commonality; they possess many local integrals of motion. These integrals of motion correspond to many symmetries within the system, which are then exploited by the Bethe ansatz in order to exactly diagonalize the system.

The ABA gives us a way to generate an infinite set of commuting operators from the Yang-Baxter algebra of an object called a *transfer matrix*. If these operators satisfy some further properties (local, self-adjoint), and one of these operators is the Hamiltonian of some system, then we have along with this Hamiltonian, an infinite set of local integrals of motion, henceforward referred to as 'conserved charges'. The self-adjoint requirement is to ensure that these operators are indeed observables, and the locality requirement comes from the nature of the Bethe ansatz; all interactions should be decomposable into local 2-particle interactions.

Now, the existence of these commuting local observables doesn't imply that they are linearly independent, so integrability isn't always implied; some further analysis needs to be done.

Our main motivation for introducing the ABA in this thesis is because it lends itself to the discussion of the conserved charges and 'integrable states' of the Lieb–Liniger model, which will be discussed in Chapter (3).

1.3.1 The Yang-Baxter Equation

We begin our description of the ABA with the introduction of what is known as the 'Yang-Baxter' equation (YBE). Given 2 copies of the same Hilbert space V_1, V_2, we want to look at operators $R(u, v)$ on the tensor space $V_1 \otimes V_2$, where u and v are complex parameters. We introduce a third copy of the Hilbert space, V_3, and use $R_{a,b}$ to mean the operator on the tensor space $V_1 \otimes V_2 \otimes V_3$ that acts like $R(u, v)$ on $V_a \otimes V_b$, and trivially on the remaining copy V_c. We say that R satisfies the Yang-Baxter equation (YBE) if:

$$R_{12}(u, v)R_{13}(u, w)R_{23}(v, w) = R_{23}(v, w)R_{13}(u, w)R_{12}(u, v). \tag{1.29}$$

For our purposes we are interested in the case when $R(u,v) = R(u-v)$. The YBE then reads

$$R_{12}(u-v)R_{13}(u-w)R_{23}(v-w) = R_{23}(v-w)R_{13}(u-w)R_{12}(u-v). \quad (1.30)$$

What kind of operators satisfy equation (1.30)? Certainly the identity operator satisfies the YBE. The permutation operators between two Hilbert spaces also offers a trivial example, ie, it is easy to check that;

$$P_{12}P_{13}P_{23} = P_{23}P_{13}P_{12}. \quad (1.31)$$

There are more examples offered in [8]. Why do we care about these R-matrices? Well to find out why, we have to first introduce the RTT or 'twist' equation.

1.3.2 The Twist Equation

Consider some operators $A(u)$, $B(u)$, $C(u)$, and $D(u)$ that act on the Hilbert space $\mathcal{H}$ of our system. We introduce a 2-dimensional auxiliary space V and construct the 'monodromy' matrix $T(u)$:

$$T(u) = \begin{pmatrix} A(u) & B(u) \\ C(u) & D(u) \end{pmatrix} \quad (1.32)$$

that acts on the space $V \otimes \mathcal{H}$. We say that $T(u)$ satisfies the RTT-relation, or the 'twist' equation if;

$$R_{12}(u-v)(T(u)\otimes\mathbb{I})(\mathbb{I}\otimes T(v)) = (\mathbb{I}\otimes T(v))(T(u)\otimes\mathbb{I})R_{12}(u-v), \quad (1.33)$$

where the space being acted on is $V_1 \otimes V_2 \otimes \mathcal{H}$, and $R_{12}(u-v)$ acts trivially on $\mathcal{H}$.

We now tie this all back to our aim: finding an infinite set of commuting operators to describe some physical, integrable system. We define the

'transfer matrix' to be:

$$\tau(u) = \mathrm{tr}(T(u)) = A(u) + D(u). \tag{1.34}$$

We can then expand $\tau(u)$ around some point u_0 in the following way:

$$\tau(u) = \sum_{i=1}^{\infty} (u - u_0)^k Q_k. \tag{1.35}$$

For reasons that will become apparent shortly, as with the choice of the R and T operators, we want to tactically choose u_0. We want to choose u_0 so that the Hamiltonian of some system we are interested in is equal to one of the Q_k. It turns out that if R is chosen to satisfy the YBE equation (1.30) and T satisfies the resulting RTT-relation, then we get that [8]:

$$[Q_n, Q_m] = 0 \qquad \forall n, m \geq 1, \tag{1.36}$$

and so we have an infinite set of commuting operators. As mentioned previously, there are some more properties that these Q_k need to satisfy to be of any use to us: they need to be local, self-adjoint, and linearly independent over $\mathbb{C}$ (or at least have an infinite linearly independent subset). If all of this is fulfilled and we set one of the Q_k to be the Hamiltonian of some quantum system, then we have found a model with an infinite set of independent conserved charges for our system, and should expect the system to thus be integrable.

1.3.3 Conserved Charges in the Lieb–Liniger Model

The construction of the monodromy and transfer matrices for the Lieb Liniger model is quite a tedious process full of calculations, and can be found in superb detail in [21]. The result is that the conserved charges are given by the following action on the Bethe states:

$$Q_k \left|\boldsymbol{\lambda}\right\rangle = \left(\sum_i \lambda_i^k\right) \left|\boldsymbol{\lambda}\right\rangle, \tag{1.37}$$

where the λ_i are the momenta describing the state $|\boldsymbol{\lambda}\rangle$. We will see later that the conserved charges of a system (specifically those invariant under spatial reflection) are important when defining the 'integrable states' of an integrable system [10]. These states only have non-zero overlaps with the parity-symmetric eigenstates of the system (the eigenstates that are invariant under spatial reflection).

Chapter 2

Bound States in Lattice Models

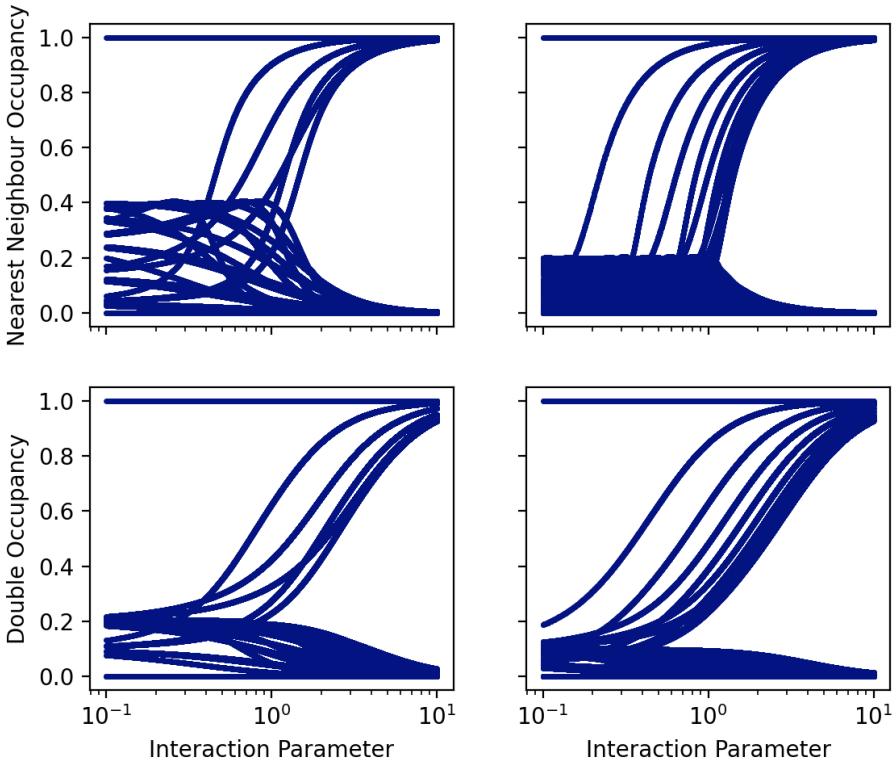

Figure 2.1: Top: Periodic XXZ (interaction parameter is Δ), Bottom: Periodic BH (interaction parameter is U) / Left: L=10, Right: L=20

In this chapter I will look at bound state occurrence in the eigenstates

of two-particle lattice models. In the Hubbard models, this means that I will be looking at double occupancy (DO) occurrence. To understand what this means for the XXZ model, we first recall the Hamiltonian of the system equation (1.3):

$$H_\Delta = -J \sum_{n=1}^{L} \left[\frac{1}{2} \left(S_n^+ S_{n+1}^- + S_n^- S_{n+1}^+ \right) + \Delta S_n^z S_{n+1}^z \right].$$

By considering a Jordan-Wigner transformation of this system [22], we can think of the Heisenberg chain as a lattice, with upspins corresponding to empty sites on the lattice, and downspins corresponding to sites occupied by fermions. The interaction parameter in this picture is now Δ.

In figure (2.1), I plot the nearest neighbour (P_{NN}) and double occupancy (P_{DO}) probabilities for the eigenstates of the 2-particle XXZ and Bose–Hubbard models, with varying numbers of sites. These probabilities are the contributions to the overall wavefunction from the position eigenstates that are nearest neighbours $\{|j, j+1\rangle \,|1 \leq j \leq L\}$ for the XXZ model, and doubly occupied $\{|j, j\rangle \,|1 \leq j \leq L\}$ for the Bose–Hubbard model. We see that there are two types of eigenstates in both cases in figure (2.1): those in which the probabilities rise to 1 at large values of the interaction parameter, and those whose probabilities drop to 0. We refer to these states in the first case as 'bound states' for obvious reasons, and those in the second case as 'unbound states'. In the first part of this chapter, I will investigate these features for the XXZ model using just momentum language. In section (2.2), I review some unpublished work done by M. Brockmann [23] on describing these features using the rapidity language of the system. In the third part, I investigate these features for the Bose–Hubbard model, and in the final part I explain why our investigation of the Bose–Hubbard model carries over explaining the features of the Fermi–Hubbard model.

2.1 XXZ Features from Momentum Language

In some situations, in order to make features of Bethe-solvable models easier to understand and explain, one re-paramaterizes the momenta of the system in a way that makes the Bethe equations more manageable. These re-paramaterized momenta are called rapidities. I will first derive a few results in canonical momentum language, and then later switch to rapidity language to see if I can obtain more results, or if the algebraic structure behind previous results becomes more clear.

Firstly, I will look at the maximum $P_{NN}(\Delta)$ a Bethe state with real momenta can have. The square norm of a Bethe wavefunction $|\psi\rangle$ with real momenta k_1 and k_2 is:

$$\langle\psi|\psi\rangle = \sum_{1\leq n_1<n_2\leq L} \left|e^{i(k_1 n_1+k_2 n_2+\frac{1}{2}\theta)} + e^{i(k_1 n_2+k_2 n_1-\frac{1}{2}\theta)}\right|^2, \tag{2.1}$$

where $\theta = \theta_{12}$ as defined in equation (1.6). Rearranging and simplifying, we get:

$$L(L-1) - 2\sum_{j=1}^{L-1}\left[(L-j)\cos\left(j\overline{k}+\theta\right)\right], \tag{2.2}$$

where $\overline{k} = k_2 - k_1$. Since the periodic chain is translationally symmetric, we only need to find $L|\langle 1,2|\psi\rangle|^2$ and divide it by the square norm to find $P_{NN}(\Delta)$. Firstly;

$$|\langle 1,2|\psi\rangle|^2 = 2(1+\cos\left(\overline{k}+\theta\right)). \tag{2.3}$$

Thus we can write $P_{NN}(\Delta)$ as:

$$\frac{2L(1+\cos\left(\overline{k}+\theta\right)}{L(L-1) - 2\sum_{j=1}^{L-1}\left[(L-j)\cos\left(j\overline{k}+\theta\right)\right]}. \tag{2.4}$$

Using a large L approximation and simplifying, we get:

$$P_{NN}(L,\Delta) = \frac{2(1+\cos\big(\overline{k}+\theta\big))}{L}. \tag{2.5}$$

Let's examine the function $\cos\big(\overline{k}+\theta\big)$. We have θ in terms of Δ, k and $\overline{k}$

from the Bethe equations:

$$\cot(\theta/2) = \frac{-\Delta \sin\big(\overline{k}/2\big)}{\cos(k/2) - \Delta \cos\big(\overline{k}/2\big)}. \tag{2.6}$$

Using this, and some trig identities, we find that $\cos \overline{k} + \theta$ is equal to:

$$\frac{2\Delta(2\cos\big(\overline{k}/2\big)\cos(k/2) - \Delta) - \cos\big(\overline{k}\big)(1+\cos(k))}{2\Delta(\Delta - 2\cos\big(\overline{k}/2\big)\cos(k/2)) + 1 + \cos(k)}. \tag{2.7}$$

For $|\Delta| \geq 1$, define the function $\Upsilon_\Delta(k, \overline{k})$ to be equal to the above expression in (2.7).

If we define new variables $u := \cos(k/2)$ and $\overline{u} := \cos\big(\overline{k}/2\big)$, our function becomes:

$$\Upsilon_\Delta(u, \overline{u}) = \frac{\Delta(2\overline{u}u - \Delta) - 2u^2\overline{u}^2 + u^2}{\Delta(\Delta - 2\overline{u}u) + u^2}. \tag{2.8}$$

where u and $\overline{u}$ are restricted to be between -1 and 1.

To maximize this function, we first analyse its gradient on its domain, namely, $[-1, 1] \times [-1, 1]$. We first solve the simultaneous equations:

1. $\partial_{\overline{u}} \Upsilon_\Delta = 0$,
2. $\partial_u \Upsilon_\Delta = 0$.

First off;

$$\partial_{\overline{u}} \Upsilon_\Delta = \frac{4u^2(\Delta u + \overline{u}^2 \Delta u - \overline{u}(\Delta^2 + u^2))}{(\Delta^2 - 2\overline{u}\Delta u + u^2)^2}. \tag{2.9}$$

So we are looking for u such that $4u^2(\Delta u + \overline{u}^2\Delta u - \overline{u}(\Delta^2 + u^2)) = 0$. There are three solutions: $u = 0$, $u = \Delta/\overline{u}$ and $u = \Delta\overline{u}$

First, if $u = 0$ then $\Upsilon_\Delta(0, \overline{u}) = -1$. This is clearly not the global maximum we are looking for as it is easy to show that our function takes on positive values on its domain. Next, if $\overline{u}$ is on the interval $[-1, 1]$ and u is equal to $\Delta/\overline{u}$, then since we are only considering cases where $|\Delta| \geq 1$, we have no solution for $u \in [-1, 1]$. This leaves us with $u = \Delta\overline{u}$. To proceed,

we must now take a look at the other partial derivative;

$$\partial_u \Upsilon_\Delta = \frac{4u\Delta(\overline{u}^2 - 1)(u\overline{u} - \Delta)}{(\Delta^2 - 2\Delta\overline{u}u + u^2)^2}. \tag{2.10}$$

Since we are considering the case $u = \Delta\overline{u}$, we are looking to solve the equation $4\overline{u}(\overline{u}^2 - 1)^2 = 0$

There are three solutions: $\overline{u} = 0$ and $\overline{u} = \pm 1$. If $\overline{u} = 0$, then u=0, and we have already investigated this case. The last two solutions fall on the boundary of the domain so we will come across them when we look at the function on the boundary of its domain.

We then move onto four one-dimensional maximization problems, ie, maximizing the following one-dimensional functions:

A. $f_1(\overline{u}) := \Upsilon_\Delta(1, \overline{u})$

B. $f_2(\overline{u}) := \Upsilon_\Delta(-1, \overline{u})$

C. $f_1(u) := \Upsilon_\Delta(u, 1)$

D. $f_2(u) := \Upsilon_\Delta(u, -1)$.

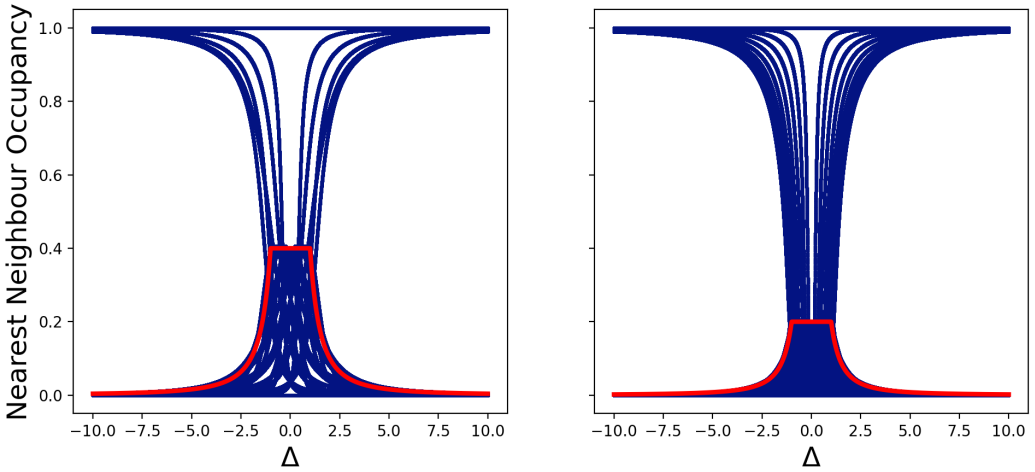

Figure 2.2: L=10 (left) and L=20 (right) nearest neighbour occupancy data (blue) plotted with max curve for real momenta (red)

The first function has one critical point in its domain at $\overline{u} = 1/\Delta$ and achieves the value $2/\Delta^2 - 1$.

The second function has one critical point in its domain at $\overline{u} = -1/\Delta$ and achieves the value $1 - 2/\Delta^2$. Note that for values of $|\Delta| \geq 1$, we get that

$$1 - 2/\Delta^2 \leq 2/\Delta^2 - 1.$$

The last two functions do not have critical points in their domain.

Lastly, we must check the edge points of the domain. All of $\Upsilon_\Delta(1,1)$, $\Upsilon_\Delta(1,-1)$, $\Upsilon_\Delta(-1,1)$, $\Upsilon_\Delta(-1,-1)$ evaluate to -1. Note that $-1 \leq 2/\Delta^2 - 1$ for all values of $|\Delta| \geq 1$.

So overall we get that for $|\Delta| \leq 1$, the maximum value of Υ_Δ is $2/\Delta^2 - 1$. Since Υ_Δ is a real cosine function ($\cos\big(\overline{k} + \theta\big)$, namely), it is always bounded above by by 1. We will use this as an upper bound for Υ_Δ when $|\Delta| \leq 1$ Therefore we get that:

$$\cos\big(\overline{k} + \theta\big) = \Upsilon_\Delta(k, \overline{k}) \leq \begin{cases} 1 & \text{if } 0 < \Delta < 1 \\ 2/\Delta^2 - 1 & \text{if } |\Delta| \geq 1. \end{cases} \tag{2.11}$$

This in turn gives us an upper bound on $P_{NN}(L, \Delta)$:

$$P_{NN}(L, \Delta) \leq \begin{cases} 4/L & \text{if } 0 < \Delta < 1 \\ 4/(L\Delta^2) & \text{if } |\Delta| \geq 1. \end{cases} \tag{2.12}$$

Graphing this curve onto our plot for the L=20 data, we see in figure (2.2) that the curve of maximum probability for states with real Bethe momenta matches up with the numerical data.

2.2 XXZ Features from Rapidity Language

We consider the same system as before, but now we will use rapidity (a re-parameterization of the momenta) language to derive some results about $P_{NN}(\Delta)$. We distinguish three different cases: planar ($|\Delta| < 1$), isotropic

($\Delta = 1$), and axial ($\Delta > 1$). We focus on the planar case which is, in our context, the most difficult one. All presented calculations can be easily transferred to the isotropic and axial cases.

Like before, the Bethe ansatz [14] yields the eigenstates of the Hamiltonian equation (1.3), which are called Bethe states. We will use the rapidities $\{\lambda_j\}_{j=1}^d$ to label the states. The rapidities in terms of the momenta of state are given below in equation (2.16).

$$|\{\lambda_j\}_{j=1}^d\rangle = \sum_{1\le n_1<\ldots<n_d\le L} |n_1,...,n_d\rangle \sum_{\sigma\in S_d} A_\sigma \prod_{j=1}^d \mathrm{e}^{ik_{\sigma_j} n_j}. \tag{2.13}$$

The amplitudes A_σ and the momenta k_i as well as the energy E of a Bethe state depend on the parameters λ_i, $i = 1, \ldots, d$, and can be written as follows:

$$A_\sigma = \mathrm{sgn}(\sigma) \prod_{\substack{i,j=1\\ i>j}}^d \exp\left(\frac{i\,\theta(\lambda_{\sigma_i} - \lambda_{\sigma_j})}{2}\right), \tag{2.14}$$

$$\theta(\lambda) = 2\arctan\left[\frac{\tanh(\lambda)}{\tan(\gamma)}\right], \tag{2.15}$$

$$k_j = k(\lambda_j), \quad k(\lambda) = -i\ln\left[\frac{\sinh\left(\lambda + \frac{i\gamma}{2}\right)}{\sinh\left(\lambda - \frac{i\gamma}{2}\right)}\right], \tag{2.16}$$

$$E = -\sum_{j=1}^d \frac{2\sin^2(\gamma)}{\sinh\left(\lambda_j + \frac{i\gamma}{2}\right)\sinh\left(\lambda_j - \frac{i\gamma}{2}\right)}, \tag{2.17}$$

where the parameter γ is related to the anisotropy via $\Delta = \cos(\gamma)$. The rapidities λ_j, $j = 1, \ldots, d$, satisfy the so-called Bethe equations

$$\left(\frac{\sinh\left(\lambda_j + \frac{i\gamma}{2}\right)}{\sinh\left(\lambda_j - \frac{i\gamma}{2}\right)}\right)^L = -\prod_{k=1}^d \frac{\sinh(\lambda_j - \lambda_k + i\gamma)}{\sinh(\lambda_j - \lambda_k - i\gamma)}. \tag{2.18}$$

There are different types of solutions of these equations [14, 24, 25], which are called strings. To find solutions to these equations in the large L limit, we note that we have two main cases:

1. The LHS of equation (2.18) has unit magnitude for either (and as a sim-

ple result, both) of the rapidities. This corresponds to both rapidities being real.

2. The LHS of equation (2.18) does not have unit magnitude for one of (and again, as an easy result, both of) the rapidities. In the large L limit, the LHS of equation (2.18) either vanishes, or diverges to infinity. If we look at the Bethe equations in this case, we get that the RHS in both cases yields either 0 or ∞, giving us two solutions;

$$\lambda_{1,2} = \lambda \pm \frac{in\pi}{2} \mp \frac{i\gamma}{2} \mp i\delta \tag{2.19}$$

where $n \in \mathbb{Z}$, but we need only consider $n = 0, 1$ for the domain of our solutions. Also, $\delta \in \mathbb{C}$ are small deviations at finite L.

We proceed first by finding the 'P_{NN}' of a general eigenstate. We do this by calculating $L\,\langle L-1, L|\psi\rangle$ (since our system is translationally symmetric) and then dividing by the norm of $|\psi\rangle$. Suppose our state $|\psi\rangle$ is given by the rapidities λ_1, λ_2. We will use $|\{\lambda_1, \lambda_2\}\rangle$ to denote this state. The 'unnormalised;' probability is given by:

$$\tilde{P}_{NN}(\lambda_1, \lambda_2, \Delta) := L|\langle L-1, L|\{\lambda_1, \lambda_2\}\rangle|^2. \tag{2.20}$$

We will then investigate the above expression for different string-type solutions. As an intermediate step we obtain

$$\tilde{P}_{NN}(\lambda_1, \lambda_2, \Delta) = L(A_{\mathrm{id}}\mathrm{e}^{-\mathrm{i}k_1} + A_{(12)}\mathrm{e}^{-\mathrm{i}k_2})\,, \tag{2.21}$$

where we used that $\mathrm{e}^{\mathrm{i}Lk_1}\mathrm{e}^{\mathrm{i}Lk_2} = 1$, which can be seen by multiplying the two Bethe equations (2.18) for λ_1 and λ_2. The two amplitudes can be written as (up to a trivial global phase)

$$A_{\mathrm{id}} = \quad (1 + \mathrm{e}^{\mathrm{i}(k_1+k_2)} - 2\Delta\mathrm{e}^{\mathrm{i}k_1})/A\,, \tag{2.22}$$

$$A_{(12)} = -(1 + \mathrm{e}^{\mathrm{i}(k_1+k_2)} - 2\Delta\mathrm{e}^{\mathrm{i}k_2})/A\,, \tag{2.23}$$

where $A = |\sin(2\gamma)K_1K_2/K_{12}|^{1/2}$ with $K_j = K_{\gamma/2}(\lambda_j)$, $K_{jk} = K_\gamma(\lambda_j - \lambda_k)$,

where $K_\alpha(\lambda) = \sin(2\alpha)/[\sinh(\lambda + \mathrm{i}\alpha)\sinh(\lambda - \mathrm{i}\alpha)]$. Using relation (2.16) for the momenta $p_{1,2}$, $\tilde{P}_{NN}(\lambda_1, \lambda_2, \Delta)$ can be further simplified to

$$\begin{aligned}\tilde{P}_{NN}(\lambda_1, \lambda_2, \Delta) &= L|\mathrm{e}^{-\mathrm{i}k_1} + \mathrm{e}^{\mathrm{i}k_2} - \mathrm{e}^{-\mathrm{i}k_2} - \mathrm{e}^{\mathrm{i}k_1}|^2/A^2 \\ &= L|\sinh(2\lambda_1)K_1 - \sinh(2\lambda_2)K_2|^2/A^2\,. \end{aligned} \tag{2.24}$$

Note that the state in equation (2.13) is not normalized. To switch from $\tilde{P}_{NN}$ to P_{NN} we have to divide by the square of the norm of a Bethe state. It is given by (up to a trivial, unimportant phase) [26, 27]

$$\mathcal{N}^2 = \det_M \left[\delta_{jk}\left(L - \sum_{l=1}^{M} K_{jl}/K_j\right) + K_{jk}/K_j\right]\,. \tag{2.25}$$

For $M = 2$ this simplifies to

$$|\mathcal{N}|^2 = |L^2 - LK_{12}(K_1^{-1} + K_2^{-1})|\,. \tag{2.26}$$

We finally obtain

$$P_{NN}(\lambda_1, \lambda_2, \Delta) = L\frac{|K_{12}|\,|\sinh(2\lambda_1)K_1 - \sinh(2\lambda_2)K_2|^2}{|\sin(2\gamma)|\,|L^2K_1K_2 - LK_{12}(K_1 + K_2)|}\,. \tag{2.27}$$

This expression is explicit in λ_1 and λ_2 and is the main result of this section. It gives the probability of finding two adjacent downspins in a Bethe state $|\{\lambda_1, \lambda_2\}\rangle$. It can be easily generalized to the axial case by replacing $\lambda \to \mathrm{i}\lambda$ and $\gamma \to \mathrm{i}\eta$ (also in the Bethe equations). To summarize, for a fixed value of Δ, i.e. $\Delta = \cos(\gamma)$ for the planar or $\Delta = \cosh(\eta)$ for the axial case, we solve Bethe equations (2.18) in order to obtain values for λ_1 and λ_2 and subsequently plug them in into equation (2.27) to compute the probability P_{NN}.

2.2.1 Real Rapidities

Let us look at the first case of solutions for (2.18). We first investigate the subset of solutions for which $\lambda_1 = -\lambda_2 = \lambda$. The first term of the

sum in the denominator of equation (2.27), which is proportional to L^2, dominates in the limit of large L the second term proportional, which is only proportional to L. This is even more pronounced for large rapidities λ. Defining $P_1(\lambda, \Delta) = P_{NN}(\lambda, -\lambda, \Delta)$ we easily find

$$P_1(\lambda, \Delta) = \frac{4\sinh^2(2\lambda)}{L(\sinh^2(2\lambda) + \sin^2(\gamma))} + \mathcal{O}(L^{-2})\,. \tag{2.28}$$

which has a γ-independent upper bound, $P_1(\lambda, \Delta) \leq 4/L$. A numerical analysis for different system sizes L (not too small) shows that states with $\lambda_1 \neq -\lambda_2$ always have smaller values $P_{NN}(\lambda_1, \lambda_2, \Delta) \leq P_1(\lambda_{\max}, \Delta)$. A generalization to $\Delta = \cosh(\eta) > 1$ is straightforward and yields

$$P_1(\lambda, \Delta) \approx \frac{4\sin^2(2\lambda)}{L(\sin^2(2\lambda) + \sinh^2(\eta))}\,. \tag{2.29}$$

However, the argument leading to an upper bound of P_1 has to be modified since the real rapidities λ_1, λ_2 are from the interval $(-\pi/2, \pi/2]$ and hence bounded for $\Delta > 1$. The expression for P_1 is maximal if $\lambda = \pi/4$. Therefore,

$$P_1(\lambda, \Delta) \leq \frac{4}{L(1 + \sinh^2(\eta))} = \frac{4}{L\Delta^2}\,. \tag{2.30}$$

Together,

$$P_1(\lambda, \Delta) \leq P_{\max} = \frac{4}{L} \begin{cases} 1 & \text{for} \quad |\Delta| \leq 1 \\ \Delta^{-2} & \text{for} \quad \Delta > 1\,. \end{cases} \tag{2.31}$$

Which is the same upper bound we got when looking at these states in the momentum picture.

2.2.2 Complex Rapidities

Let us now consider the second case of solutions for (2.18). For any even L there is one special solution of (2.19) with $n = 0$, for which λ and the deviation δ are exactly zero. The corresponding Bethe equations are singular.

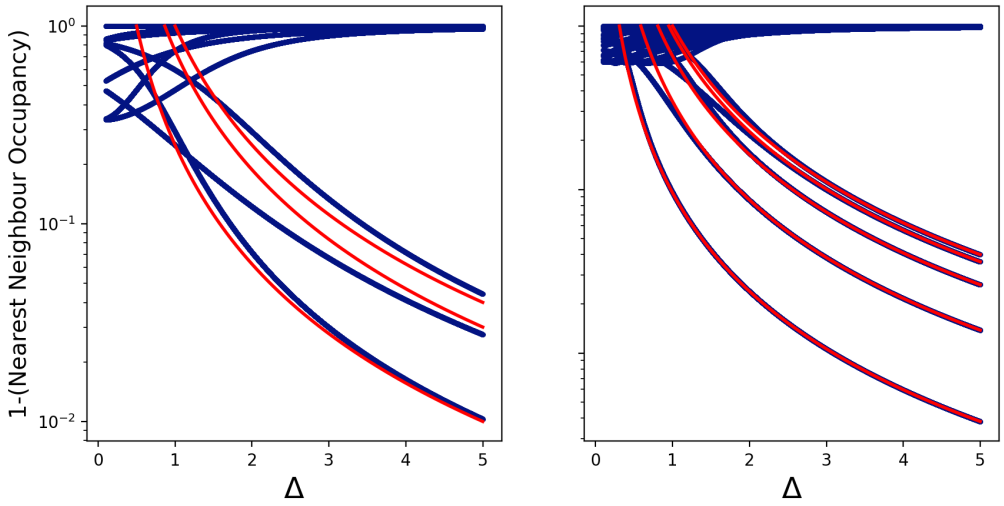

Figure 2.3: Numerical results (blue) plotted with $P_2^{(n)}$ (red) from $\Delta = \Delta_n$ to $\Delta = 5$. $L = 6$ on the left and $L = 10$ on the right

However, the state can be computed as [14, 28, 29]

$$|\{\mathrm{i}\gamma/2, -\mathrm{i}\gamma/2\}\rangle = \frac{1}{\sqrt{L}} \sum_{j=1}^{L} (-1)^j \, |j, j+1\rangle \, . \tag{2.32}$$

It easily follows that $P_{NN}(\mathrm{i}\gamma/2, -\mathrm{i}\gamma/2, \Delta) = 1$, which is independent of anisotropy Δ. The other solutions can be treated as follows. For large L the deviation δ is exponentially small and hence $K_{12} \approx -1/\sin(2\delta)$. Therefore, the second term of the sum in the denominator of equation (2.27) dominates. The sum $K_1 + K_2$ can be computed in the limit $\delta \to 0$ as

$$K_1 + K_2 = K_{\frac{\gamma}{2}}(\lambda + \tfrac{\mathrm{i}\gamma}{2}) + K_{\frac{\gamma}{2}}(\lambda - \tfrac{\mathrm{i}\gamma}{2}) = K_\gamma(\lambda) \, , \tag{2.33}$$

and the difference in the numerator yields

$$\sinh(2\lambda + \mathrm{i}\gamma) K_1 - \sinh(2\lambda - \mathrm{i}\gamma) K_2 = \sin(\gamma) K_\gamma(\lambda) \, . \tag{2.34}$$

Together, defining $P_2(\lambda, \Delta) = P_{NN}(\lambda + \frac{\mathrm{i}\gamma}{2}, \lambda - \frac{\mathrm{i}\gamma}{2}, \Delta)$ for 2-string states, we obtain

$$P_2(\lambda, \Delta) = \frac{\sin^2(\gamma) K_\gamma(\lambda)}{\sin(2\gamma)} = \frac{\sin^2(\gamma)}{\sinh^2(\lambda) + \sin^2(\gamma)} \,. \tag{2.35}$$

Using $\Delta = \cos(\gamma)$ and some trigonometric relations, this result can be also expressed in terms of the energy E and the total momentum $k = k_1 + k_2$ of the 2-string state [7],

$$\begin{aligned} P_2(\Delta) &= -\frac{E}{4\Delta} = -\frac{1}{4\Delta}\frac{\sin(\gamma)}{\sin(2\gamma)}(\cos(k) - \cos(2\gamma)) \\ &= 1 - \frac{\cos^2(k/2)}{\Delta^2} \,. \end{aligned} \tag{2.36}$$

From the condition $P_2 \geq 0$ the end points of the different branches $P_2^{(n)} = P_2(\lambda(k_n), \Delta)$, $k_n = \pi - 2\pi n/L$, $n = -L/2 + 1, \ldots, L/2$, as function of anisotropy can be derived: $\Delta \geq \Delta_n = |\sin(\pi n/L)|$. The generalization to $\Delta \geq 1$ is straightforward and yields exactly the same expression (2.36). The branches $P_2^{(n)}$ with their endpoints Δ_n are shown in figure (2.3) for $L = 6, 10$. Note that the branch $P_2^{(n)}$ is degenerate with $P_2^{(L-n)}$ for all $n = 1, \ldots, L/2$. The branch $P_2^{(0)} = 1$, i.e. $k = \pi$ or $\lambda = 0$, corresponds to the aforementioned special solution $\lambda_1 = -\lambda_2 = i\gamma/2$ and gives an upper bound for $P_2(\Delta)$, whereas $n = L/2$, i.e. a 2-string with center at $\pi/2$ corresponding to total momentum $k = 0$, gives a lower bound, $P_2(\Delta) \geq 1 - 1/\Delta^2$ for all $\Delta \geq 1$.

2.3 Bose–Hubbard Features from Momentum Language

Here we move on to look at the Bose Hubbard model with two bosons in L sites. Recall the Hamiltonian from equation (1.14):

$$H_{BH} = \sum_{0 \leq i \leq L} \left(b_i^\dagger b_{i+1} + b_i b_{i+1}^\dagger \right) + \frac{U}{2} \sum_{i=1}^{L} n_i(n_i - 1).$$

In section (2.3) we found that the eigenstates of this Hamiltonian are of the form:

$$|\Psi\rangle = \sum_{1\leq n_1\leq n_2\leq L} \left(e^{i(k_1 n_1 + k_2 n_2)} + e^{i(k_1 n_2 + k_2 n_1 + \theta)}\right) |n_1, n_2\rangle \,, \tag{2.37}$$

where the Bethe equations for the model are:

$$e^{i\theta} = \frac{\sin(k_1) - \sin(k_2) - iU/2}{\sin(k_1) - \sin(k_2) + iU/2}. \tag{2.38}$$

We can rewrite this using $k = k_1 + k_2$ and $\overline{k} = k_2 - k_1$:

$$e^{i\theta} = \frac{2\cos(k/2)\sin\left(\overline{k}/2\right) + iU/2}{2\cos(k/2)\sin\left(\overline{k}/2\right) - iU/2}. \tag{2.39}$$

We now turn our attention to finding the maximum of the 'Double Occupancy' probability for eigenstates where both bosons have real momenta. This comes down to calculating:

$$\frac{\sum_{i=1}^{L} \langle i, i|\Psi\rangle^2}{\langle\Psi|\Psi\rangle} = \frac{L\,\langle 1, 1|\Psi\rangle^2}{\langle\Psi|\Psi\rangle}. \tag{2.40}$$

due to translational symmetry thanks to the periodic boundary conditions. Now;

$$\langle 1, 1|\Psi\rangle^2 = |e^{i(k_1+k_2)} + e^{i\theta}e^{i(k_2+k_1)}|^2 = |e^{ik}|^2|1 + e^{i\theta}|^2 = |1 + e^{i\theta}|^2$$

as k is real, and:

$$\begin{aligned}\langle\Psi|\Psi\rangle &= \sum_{1\leq n_1\leq n_2\leq L} |e^{i(k_1 n_1 + k_2 n_2 + \theta)} + e^{i(k_1 n_2 + k_2 n_1)}|^2 \\ &= 2\sum_{1\leq n_1\leq n_2\leq L} \left(1 + \cos\left((n_1 - n_2)\overline{k} - \theta\right)\right). \end{aligned} \tag{2.41}$$

We get that for large L approximation;

$$\langle\Psi|\Psi\rangle \approx 2L^2 \tag{2.42}$$

and so:

$$P_{DO}(L,U) \approx \frac{1+\cos(\theta)}{L}. \tag{2.43}$$

Now we need to find the maximum of this function. It should be clear that we need to maximize the cosine function in the above expression. We know that $\cos(\theta) = \mathrm{Re}(e^{i\theta})$ and so;

$$\begin{aligned}\cos(\theta) &= \mathrm{Re}\left(\frac{2\cos(k/2)\sin(\overline{k}/2) + iU/2}{2\cos(k/2)\sin(\overline{k}/2) - iU/2}\right) \\ &= \frac{4\cos^2(k/2)\sin^2(\overline{k}/2) - U^2/4}{4\cos^2(k/2)\sin^2(\overline{k}/2) + U^2/4}\end{aligned} \tag{2.44}$$

as k and $\overline{k}$ are both real.
We are looking to maximize the function;

$$\Upsilon_U : [0,1]\times[0,1] \longrightarrow \mathbb{R} : (x,y) \longmapsto \frac{4xy - U^2/4}{4xy + u^2/4}. \tag{2.45}$$

This function has no critical points on its interior, and obtains a global max at $x = y = 1$;

$$\Upsilon_{U,\max} = \frac{4 - U^2/4}{4 + U^2/4} = \frac{16 - U^2}{16 + U^2}, \tag{2.46}$$

which gives us the following result;

$$P_{DO}(L,U) \leq \frac{32}{L(16+U^2)}. \tag{2.47}$$

We plot this maximum curve against the L=20 data in figure (2.4).

2.4 Brief Discussion of the Fermi–Hubbard model

Recall the Hamiltonian from equation (1.15):

$$H_{FH} = \sum_{\sigma\in\{\uparrow\downarrow\}} \sum_{0\leq i\leq L} \left(c^\dagger_{i,\sigma}c_{i+1,\sigma} + c_{i,\sigma}c^\dagger_{i+1,\sigma}\right) + \frac{U}{2}\sum_{i=1}^{L} n_{i\uparrow}n_{i\downarrow}.$$

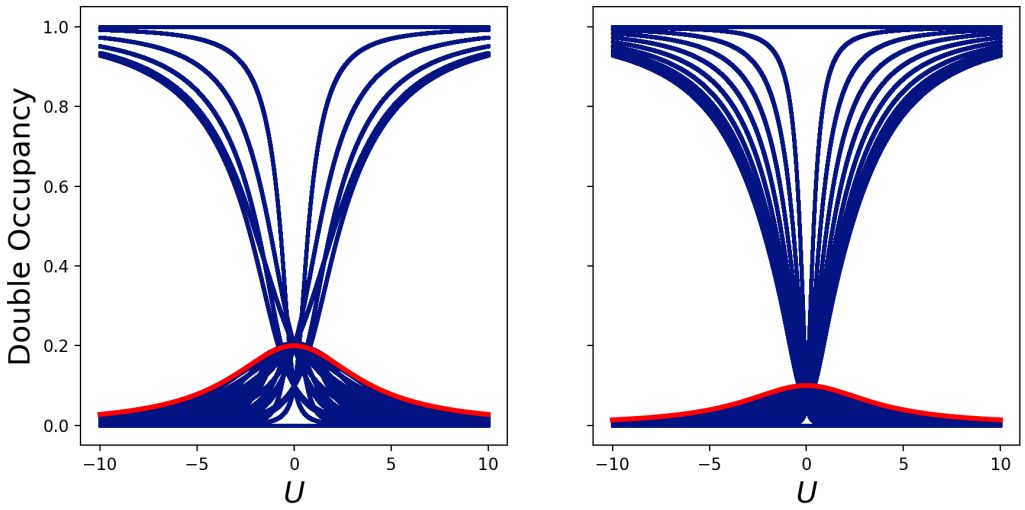

Figure 2.4: L=10 (left) and L=20 (right) double occupancy data (blue) plotted with max curve for real momenta (red)

H_{FH} can be block diagonalized over our Hilbert space $\mathcal{H} = \mathcal{H}_1 \bigoplus \mathcal{H}_2$ where $\mathcal{H}_1$ has basis:

$$\mathcal{B}_1 = \{|n_\sigma, m_\sigma\rangle \,|1 \leq n < m \leq L, \sigma \in \{\uparrow, \downarrow\}\}, \tag{2.48}$$

and $\mathcal{H}_2$ has basis:

$$\mathcal{B}_2 = \{|n_\sigma, m_{\overline{\sigma}}\rangle \,|1 \leq n \leq m \leq L, \sigma \in \{\uparrow, \downarrow\}\} \tag{2.49}$$

(where $\overline{\uparrow} = \downarrow$ and $\overline{\downarrow} = \uparrow$).
This block diagonal action comes from the fact that H_{FH} contains no spin flips.

If we put H_{FH} into block diagonal form $H_{FH} = H_1 \bigoplus H_2$ where H_1 acts on $\mathcal{H}_1$ and H_2 acts on $\mathcal{H}_2$, then it should be clear that the double occupancy probability of any state in $\mathcal{H}_1$ is always zero. So we are only interested in the space $\mathcal{H}_2$.

If we take a look at $\mathcal{H}_2$, we notice it has dimension L^2. We define a new

basis $\mathcal{B}_2'$ for $\mathcal{H}_2$:

$$\mathcal{B}_2' = \mathcal{B}_2^+ \sqcup \mathcal{B}_2^- \sqcup \mathcal{B}_2^0, \tag{2.50}$$

where

$$\mathcal{B}_2^+ = \left\{ \frac{1}{\sqrt{2}} \left(|n_\uparrow, m_\downarrow\rangle + |n_\downarrow, m_\uparrow\rangle \right) \middle| 1 \leq n < m \leq L \right\}, \tag{2.51}$$

$$\mathcal{B}_2^- = \left\{ \phi_{nm} = \frac{1}{\sqrt{2}} \left(|n_\uparrow, m_\downarrow\rangle - |n_\downarrow, m_\uparrow\rangle \right) \middle| 1 \leq n < m \leq L \right\}, \tag{2.52}$$

and

$$\mathcal{B}_2^0 = \left\{ \phi_{nn} = |n_\uparrow, n_\downarrow\rangle \middle| 1 \leq n \leq L \right\}. \tag{2.53}$$

It can easily be shown that H_2 can be block–diagonalized via actions on the subspaces $\mathrm{Sp}(\mathcal{B}_2^+)$ and $\mathrm{Sp}(\mathcal{B}_2^0 \cup \mathcal{B}_2^-)$. We can thus write H_2 as the block diagonal sum $H_2^+ \bigoplus H_2^{-,0}$ which act respectively on the two subspaces mentioned above. Looking at $\mathcal{B}_2^+$, it should be clear that all states in $\mathrm{Sp}(\mathcal{B}_2^+)$ always have zero double occupancy probability. We thus turn our attention purely to $\mathrm{Sp}(\mathcal{B}_2^0 \cup \mathcal{B}_2^-)$.

We first notice that the dimension of the Hilbert space $\mathrm{Span}(\mathcal{B}^- \cup \mathcal{B}^0)$ is $L(L+1)/2$, which is the same as the dimension of the Hilbert space for the Bose Hubbard model with 'L' sites. Furthermore, if we define $\psi_{nm} = b_n^\dagger b_m^\dagger |\mathrm{vac}\rangle$ where $n \leq m$ for basis states of our Bose–Hubbard model in equation (1.14), then it is easily verified that:

$$\langle \psi_{n'm'} | \, H_{BH} \, | \psi_{nm} \rangle = \langle \phi_{n'm'} | \, H_2^{-,0} \, | \phi_{nm} \rangle \,, \tag{2.54}$$

where the ϕ's are defined above.

As a result, it follows that the Double-Occupancy probabilities for the Fermi–Hubbard model follow those of the Bose–Hubbard model, with the extra $L(L-1)$ extra states that we disregarded earlier having constant zero

probability. I verified directly that this indeed the case.

2.5 Conclusion

In this chapter, I showed that the Bethe ansatz can be used to describe bound state occurrence in the 2-particle sector of various integrable 1D lattice models. I found contrasting expressions for the maximum 'bound state probability' curve for real momenta in the XXZ and Bose Hubbard models, namely:

$$P_{NN}(L,\Delta) \leq \begin{cases} 4/L & \text{if } 0 < \Delta < 1 \\ 4/(L\Delta^2) & \text{if } |\Delta| \geq 1 \end{cases}$$

for the XXZ, and

$$P_{DO}(L,U) \leq \frac{32}{L(16+U^2)}$$

for the Bose–Hubbard.

Also, rapidity language was used to re-derive the above expression for the XXZ model, as well as fully characterise the 'bound state probability' curves that rise to 1 as $|\Delta| \to \infty$ in equation (2.36).

Finally, I showed that my analysis of the bound state probabilities in the Bose–Hubbard model was sufficient to fully describe those in the Fermi–Hubbard model. Although the Hilbert space of the Fermi–Hubbard model is larger than that of the Bose–Hubbard model, we are able to split the Fermi–Hubbard Hilbert space into two. The bound state probabilities of the first subspace is constantly zero for all states (due to the Pauli exclusion principle), and the bound state probabilities of the second subspace are identical to those of the Bose–Hubbard model.

Apart from the unsolvability of the Bose–Hubbard model by the Bethe ansatz for more than two particles, it is not clear how to define analogous bound states in these models with more than two particles. Do we look for contributions from position eigenstates in which just two particles are 'bound' (nearest neighbour/double occupancy)? Or maybe we want all the

particles on the lattice to be 'bound'? This needs to be decided before these results are studied in the fixed density thermodynamic limit.

Chapter 3

Quench Overlaps in the Lieb–Liniger Model

In this chapter I will present calculations of the overlaps of two different 'rotating' Bose-Einstein condensates with parity-symmetric eigenstates of the Lieb–Liniger model. I start the chapter with some background and motivation for these calculations. The main motivation is for the use of these overlaps in various 'quenching' scenarios (using the quench action [30] to time-evolve local operators, for example). I then introduce the 'conserved charges' of the Lieb–Liniger model (see section (1.3.3)), and how I use these (along with the parity-symmetric eigenstates) to introduce the 'integrable states' [10] of our system. I then begin the calculation with the 2-particle case. I use this to then guide the method of calculation for the general N-particle case. I finish the chapter with a short comparison of the overlaps for the two different BECs.

3.1 The Quench Method

We will begin this chapter by introducing the notion of 'quenches' [30, 31] in quantum systems. The main idea stems from seeing how a 'generic' initial

state $|\psi(t)\rangle$ evolves under a given Hamiltonian:

$$|\psi(t)\rangle = e^{-iHt} |\psi(t=0)\rangle \,. \tag{3.1}$$

How does one generate a 'generic' initial state? First of all, we obviously don't want to pick an eigenstate of H as this has trivial evolution under the unitary operator e^{-iHt}. Instead we want a state that is almost certainly **not** an eigenstate of H. One way to do this is to vary the interaction parameter in the Hamiltonian (if it has one).

To demonstrate this, let $|\psi_0\rangle$ be an eigenstate of our free Hamiltonian H_0. We then choose a value of our interaction parameter $|c| > 0$ and expand $|\psi_0\rangle$ in the eigenbasis of this new Hamiltonian H with eigenbasis $\{\phi\}$:

$$|\psi_0\rangle = \sum_{\phi} \langle\phi|\psi_0\rangle \, |\phi\rangle = \sum_{\phi} e^{-S_\phi} \, |\phi\rangle \,, \tag{3.2}$$

where $S_\phi = -\ln \langle\phi|\psi_0\rangle$. We can now easily evolve $|\psi_0\rangle$ under the Hamiltonian with interaction:

$$e^{-iHt} \, |\psi_0\rangle = \sum_{\phi} e^{-S_\phi - i\varepsilon_\phi t} \, |\phi\rangle \,, \tag{3.3}$$

where ε_ϕ is the eigenenergy corresponding to the Bethe state $|\phi\rangle$. So one can see that these overlaps are key to calculating the time evolution of operators acting on a generic state.

For example, recall the Lieb–Liniger Hamiltonian equation (1.18):

$$H_c = -\sum_{j=1}^{N} \frac{\partial^2}{\partial x_j^2} + 2c \sum_{j<l} \delta(x_j - x_l). \tag{3.4}$$

We could look at the free Hamiltonian $H_{c=0}$ for $t < 0$ and choose an eigenstate of this Hamiltonian. Then at $t = 0$, we instantaneously switch on interaction to some value $|c| > 0$. This eigenstate of the free Hamiltonian will clearly not be an eigenstate of our new Hamiltonian with interactions turned on.

3.2 Conserved Charges and Integrable States

Let $\{Q_l\}_{l\in\mathbb{N}}$ be the set of conserved charges of the Lieb–Liniger Hamiltonian (recall conserved charges of a Bethe system from section (1.3.3)). The action of the Q_l's on the Bethe states is simple:

$$Q_l \left|\lambda_1, ..., \lambda_N\right\rangle = \left(\sum_{j=1}^{N} \lambda_j^l\right) \left|\lambda_1, ..., \lambda_N\right\rangle . \tag{3.5}$$

Note: It's easy enough to show that $|\boldsymbol{\lambda}\rangle$ is parity symmetric $\iff Q_{2l+1}|\boldsymbol{\lambda}\rangle = 0$ for all l.

We say a state $|\psi\rangle$ is integrable [10] if all conserved charges that are odd under spatial reflection annihilate it:

$$Q_{2l+1}|\psi\rangle = 0, \qquad l = (0, 1, 2, ...).$$

Say we have an integrable state $|\psi\rangle$ and define $\alpha_l = \sum_{j=1}^{N} \lambda_j^{2l+1}$. Then:

$$\alpha_l \langle\psi|\boldsymbol{\lambda}\rangle = \langle\psi|Q_{2l+1}\boldsymbol{\lambda}\rangle = \langle\boldsymbol{\lambda}|Q_{2l+1}\psi\rangle^* = 0.$$

We have two cases:

1. If $|\boldsymbol{\lambda}\rangle$ is parity symmetric, $\alpha_l = 0$ for all l, and thus $\langle\psi|\boldsymbol{\lambda}\rangle$ can be non-zero.

2. If $|\boldsymbol{\lambda}\rangle$ is non-parity symmetric, then there exists l such that α_l is non zero, and thus $\langle\psi|\boldsymbol{\lambda}\rangle = 0$.

If instead $|\psi\rangle$ is not an integrable state, then we no longer get the requirement that $\langle\psi|\boldsymbol{\lambda}\rangle = 0$ when $|\boldsymbol{\lambda}\rangle$ is non-parity symmetric.

Let's continue the discussion of conserved charges and integrable states. For lattice models, typically Q_j is a sum along the chain of local operators spanning j sites, so Q_j is only physically meaningful for $j < N$ where N is the total number of sites, and thus to check if a state is integrable, one only needs to check the action of Q_{2l+1} on $|\psi\rangle$ for $2l + 1 \leq N$.

In our case, in order to show that, we need only check Q_{2l+1} for $2l+1 < N$ to determine whether a state is integrable, it is sufficient to show that if we define $p_l(\boldsymbol{z}) = \sum_j z^l$ as the l-th power sum of some complex variables $z_1, ..., z_N$ where N is even, then:

$$p_{2l+1}(\boldsymbol{z}) = 0 \quad \forall\, 2l+1 < N \implies p_{2l'+1}(\boldsymbol{z}) = 0 \quad \forall\, 2l'+1 > N. \tag{3.6}$$

The proof of this is given in appendix A.

3.3 Overlaps with Parity Symmetric States

We now look at the overlaps of 2 specific counter-rotating BECs [32, 33] with parity-symmetric Bethe states, ie, Bethe States whose momenta come in opposite-sign pairs: $|\boldsymbol{\lambda_N}\rangle = \left|\boldsymbol{\lambda_{N/2}}, -\boldsymbol{\lambda_{N/2}}\right\rangle$. I will be using methods found in [33] and [34]. What I will hopefully illustrate, is that these two initial states are actually the same - provided we project them onto the space spanned by these parity symmetric Bethe states. A quick note: while I was working on this problem, the (at the time, pre-print, but now fully published paper) [33] was updated to include this very calculation for one of the initial BEC states I was looking at. This new calculation for the other initial state however, is to my knowledge new, as is the comparison between the two BEC states.

3.3.1 The BEC Initial States

We first begin by writing the oppositely-rotating BEC in 2nd quantization. In this form we can easily see how both BECs achieve bosonic symmetry in different ways.

The counter-rotating BEC takes the form:

$$|\psi_1\rangle = \frac{1}{2^{N/2}}(a_k^\dagger + a_{-k}^\dagger)^N |0\rangle\,, \tag{3.7}$$

while the fragmented BEC in 2nd quantization looks like:

$$|\psi_2\rangle = (a_k^\dagger)^{N/2}(a_{-k}^\dagger)^{N/2}\,|0\rangle\,. \tag{3.8}$$

Note that $|\psi_1\rangle$ can be constructed for the Lieb–Liniger model for any number of bosons, while $|\psi_2\rangle$ requires that we have an even number of bosons.

For calculations in this manuscript, we'll need to use first quantization:

$$\langle \boldsymbol{x}|\psi_1\rangle = \frac{1}{\sqrt{(2L)^N}}\prod_{i=1}^{N}\left(e^{ikx_i}+e^{-ikx_i}\right), \tag{3.9}$$

$$\langle \boldsymbol{x}|\psi_2\rangle = \frac{1}{(N/2)!\sqrt{N!L^N}}\sum_{\sigma\in S_N} e^{i\boldsymbol{k}\cdot\sigma\boldsymbol{x}}, \tag{3.10}$$

where $\boldsymbol{k}=\{+k,-k,...,+k,-k\}$. I will use C_N^ψ to mean the relevant normalization factors for a state $|\psi\rangle$ above. For $|\psi_1\rangle$ it will mean $1/\sqrt{(2L)^N}$ and for $|\psi_2\rangle$ it will mean $1/[(N/2)!\sqrt{N!L^N}]$.

3.3.2 The Bethe States of Our System with Interaction

The calculations of the Bethe states for the Lieb–Liniger model can be found in section (1.2.3). I will write the main results here:

$$\langle \boldsymbol{x_N}|\boldsymbol{\lambda_N}\rangle = \frac{c^{N/2}}{\sqrt{N!}}\sum_{\sigma\in S_N} A_\sigma \exp\left(i\sum_j \lambda_{\sigma(j)}x_{\sigma(j)}\right)\prod_{j>l}, \tag{3.11}$$

where:

$$A_\sigma = \prod_{j>l}\left(1-\frac{ic\ \mathrm{sgn}(x_j-x_l)}{\lambda_{\sigma(j)}-\lambda_{\sigma(l)}}\right). \tag{3.12}$$

The norms of these states are given by the Gaudin formula [27]:

$$\langle \lambda_N|\lambda_N\rangle = c^N\prod_{j\neq l} f(\lambda_j,\lambda_l)\det G, \tag{3.13}$$

where G is given by:

$$G_{jk} = \delta_{jk}\left(L + \sum_{l=1}^{N}\varphi(\lambda_j - \lambda_l)\right) - \varphi(\lambda_j - \lambda_k), \tag{3.14}$$

$f(\lambda_1, \lambda_2)$ is given by:

$$f(\lambda_1, \lambda_2) = \frac{\lambda_1 - \lambda_2 + ic}{\lambda_1 - \lambda_2}, \tag{3.15}$$

and $\varphi(\lambda)$ is given by:

$$\varphi(\lambda) = \frac{2c}{\lambda^2 + c^2}. \tag{3.16}$$

3.3.3 Parity Symmetric Bethe States

We can further simplify the expression for the norm of a Bethe state if we assume that the state is parity symmetric [33]:

$$|\boldsymbol{\lambda_N}\rangle = |\lambda_1^+, -\lambda_1^+, ..., \lambda_{N/2}^+, -\lambda_{N/2}^+\rangle = |\boldsymbol{\lambda}_{N/2}^+, -\boldsymbol{\lambda}_{N/2}^+\rangle\,. \tag{3.17}$$

The norm in this case $||\,|\boldsymbol{\lambda}_{N/2}^+, -\boldsymbol{\lambda}_{N/2}^+\rangle\,||^2$ can be written as:

$$c^N \prod_{j=1}^{N/2} f(\lambda_j^+, -\lambda_j^+) f(-\lambda_j^+, \lambda_j^+) \prod_{1\le j<k\le N/2} [\overline{f}(\lambda_j^+, \lambda_k^+)]^2 \det G^+ \det G^-, \tag{3.18}$$

where:

$$\overline{f}(\lambda_j^+, \lambda_k^+) = f(\lambda_j^+, \lambda_k^+) f(\lambda_j^+, -\lambda_k^+) f(\lambda_j^+, -\lambda_k^+) f(-\lambda_j^+, -\lambda_k^+), \tag{3.19}$$

and $G^{\pm}$ are $N/2 \times N/2$ matrices given by:

$$G_{jk}^{\pm} = \delta_{jk}\left[L + \sum_{l=1}^{N/2}\varphi^+(\lambda_j^+, \lambda_l^+)\right] - \varphi^{\pm}(\lambda_j^+, \lambda_k^+). \tag{3.20}$$

3.3.4 Explicit Overlap calculation for N=2

Let $|\psi\rangle$ be one of $|\psi_1\rangle$, $|\psi_2\rangle$, and let $\mathbf{1}$ be the simplex given by $0 < x_1 < x_2 < L$. The overlap of the unnormalized Bethe state $|\lambda_1, \lambda_2\rangle$ with the BEC initial state $|\psi\rangle$ takes the following form:

$$\frac{2c}{\sqrt{2}C_2^\psi} \sum_{\substack{\sigma\in S_2 \\ \mathbf{s}\in \mathrm{Sgn}_2^\psi}} f(\lambda_{\sigma_1}, \lambda_{\sigma_2}) \int_{\mathbf{1}} \mathrm{d}x_2 \mathrm{d}x_1 \exp\left[i \sum_j (\lambda_{\sigma_j} + s_j k) x_j \right], \tag{3.21}$$

where C_N^ψ is the normalisation factor associated to the BEC state $|\psi\rangle$ with N particles, and Sgn_N^ψ is a subset of $\{\pm\}^N$ that depends on the choice of initial state $|\psi\rangle$. For example, using the definitions of $|\psi_{1,2}\rangle$ from equations (3.9), (3.10), we have that $\mathrm{Sgn}_2^1 = \{(+,-),(-,+)\}$ and $\mathrm{Sgn}_2^2 = \{\pm\} \times \{\pm\}$.

Next, it is useful to introduce the following integral:

$$B_N(\alpha_1, ..., \alpha_N) = \int_{\mathbf{1}} \mathrm{d}x_N \mathrm{d}x_{N-1} ... \mathrm{d}x_1 \exp\left[i \sum_j \alpha_j x_j \right]. \tag{3.22}$$

We can easily calculate this for $N = 2$:

$$\begin{aligned} B_2(\alpha_1, \alpha_2) &= \int_0^L \mathrm{d}x_2 \int_0^{x_2} \mathrm{d}x_1 \exp\left[i(\alpha_1 x_1 + \alpha_2 x_2) \right] && (3.23) \\ &= \frac{1}{i\alpha_1} \int_0^L \mathrm{d}x_2 \left[\exp\left[i x_2 (\alpha_1 + \alpha_2) \right] - \exp\left[i\alpha_2 x_2 \right] \right] && (3.24) \\ &= \frac{1}{i\alpha_1} \left[\frac{e^{iL(\alpha_1+\alpha_2)} - 1}{i(\alpha_1 + \alpha_2)} - \frac{e^{iL\alpha_2} - 1}{i\alpha_2} \right]. && (3.25) \end{aligned}$$

Substituting $\lambda_{\sigma_j} + s_j k$ for α_j we get the following expression for $B(\lambda_{\sigma_1} + s_1 k, \lambda_{\sigma_2} + s_2 k)$:

$$\frac{1}{i\lambda_{\sigma_1} + s_1 k} \left[\frac{e^{iL(\lambda_{\sigma_1} + s_1 k + \lambda_{\sigma_2} + s_2 k)} - 1}{i(\lambda_{\sigma_1} + s_1 k + \lambda_{\sigma_2} + s_2 k)} - \frac{e^{iL(\lambda_{\sigma_2} + s_2 k)} - 1}{i\lambda_{\sigma_2} + s_2 k} \right]. \tag{3.26}$$

Since k is quantised via the periodic boundary condition $e^{ikL} = 1$ we can

rewrite the above expression as:

$$\frac{1}{i(\lambda_{\sigma_1}+s_1k)}\left[\frac{e^{iL(\lambda_{\sigma_1}+\lambda_{\sigma_2})}-1}{i(\lambda_{\sigma_1}+\lambda_{\sigma_2}+(s_1+s_2)k)}-\frac{e^{iL\lambda_{\sigma_2}}-1}{i(\lambda_{\sigma_2}+s_2k)}\right]. \tag{3.27}$$

I claim (due to momentum conservation) that the only non-zero terms in the $s=\pm$ sum after the parity limit $\lambda_2\to-\lambda_1=-\lambda$ is taken are those where the number of λ_+k match the number of λ_-k. I will show this explicitly for the $N=2$ case. So we will consider a term where $s_1=s=s_2$, and then take the parity invariant Bethe state $\lambda_2\to-\lambda_1$. We must calculate the sum:

$$\sum_{\sigma\in S_2} f(\lambda_{\sigma_1},\lambda_{\sigma_2})B(\lambda_{\sigma_1}+sk,\lambda_{\sigma_2}+sk). \tag{3.28}$$

First note that we can simplify $B(\lambda_{\sigma_1}+sk,\lambda_{\sigma_2}+sk)$ to get:

$$\frac{1}{i(\lambda_{\sigma_1}+sk)}\left[\frac{e^{iL(\lambda_{\sigma_1}+\lambda_{\sigma_2})}-1}{i(\lambda_{\sigma_1}+\lambda_{\sigma_2}+2sk)}-\frac{e^{iL\lambda_{\sigma_2}}-1}{i(\lambda_{\sigma_2}+sk)}\right]. \tag{3.29}$$

Note that when we take $\lambda_{\sigma_2}\to-\lambda_{\sigma_1}$ the first term vanishes and we get:

$$B(\lambda_{\sigma_1}+sk,\lambda_{\sigma_2}+sk)=\frac{e^{-iL\lambda_{\sigma_1}}-1}{(\lambda_{\sigma_1}+sk)(-\lambda_{\sigma_1}+sk)}. \tag{3.30}$$

So we can now calculate equation (3.28):

$$\sum_{\sigma\in S_2} f(\lambda_{\sigma_1},\lambda_{\sigma_2})B(\lambda_{\sigma_1}+sk,\lambda_{\sigma_2}+sk)= \frac{1}{(\lambda_1+sk)(-\lambda_1+sk)}\left[f(\lambda_1,\lambda_2)(a_2-1)+f(\lambda_2,\lambda_1)(a_1-1)\right] \tag{3.31}$$

where we defined $a_j=e^{i\lambda_jL}$.

Now, we know that the Bethe equations can be written as [20]:

$$a_j = \prod_{l \neq j} \frac{f(\lambda_j, \lambda_l)}{f(\lambda_l, \lambda_j)}, \tag{3.32}$$

so equation (3.31) can be written as

$$\frac{1}{(\lambda_{\sigma_1} + sk)(-\lambda_{\sigma_1} + sk)} \times \left[f(\lambda_1, \lambda_2) \left(\frac{f(\lambda_2, \lambda_1)}{f(\lambda_1, \lambda_2)} - 1 \right) + f(\lambda_2, \lambda_1) \left(\frac{f(\lambda_1, \lambda_2)}{f(\lambda_2, \lambda_1)} - 1 \right) \right], \tag{3.33}$$

which vanishes as expected, so we need only calculate the $(+,-),(-,+)$ terms in the '$\mathbf{s}$' sum. More generally for larger N later, we need only care about the subset $\{\mathbf{s} \in \mathrm{Sgn}_\psi | \sum_j s_j = 0\}$ when we sum over Sgn_ψ. Now onto the case where $s_1 = s = -s_2$. We must find the sum:

$$\sum_{\sigma \in S_2} f(\lambda_{\sigma_1}, \lambda_{\sigma_2}) B(\lambda_{\sigma_1} + sk, \lambda_{\sigma_2} - sk). \tag{3.34}$$

We first calculate the B term:

$$B(\lambda_{\sigma_1} + sk, \lambda_{\sigma_2} - sk) = \frac{1}{i(\lambda_{\sigma_1} + sk)} \left[\frac{e^{iL(\lambda_{\sigma_1} + \lambda_{\sigma_2})} - 1}{i(\lambda_{\sigma_1} + \lambda_{\sigma_2})} - \frac{e^{iL\lambda_{\sigma_2}} - 1}{i(\lambda_{\sigma_2} - sk)} \right]. \tag{3.35}$$

Taking $\lambda_{\sigma_2} \to -\lambda_{\sigma_1}$ we must be careful of the pole in the first term. We expand the numerator to linear order in $\lambda_{\sigma_1} + \lambda_{\sigma_2}$ and get a cancellation on top and bottom. We can thus write equation (3.35) as:

$$\frac{1}{i(\lambda_{\sigma_1} + sk)} \left[L - \frac{e^{iL\lambda_{\sigma_2}} - 1}{i(\lambda_{\sigma_2} - sk)} \right] = \frac{1}{i(\lambda_{\sigma_1} + sk)} \left[L + \frac{a_{\sigma_2} - 1}{i(\lambda_{\sigma_1} + sk)} \right]. \tag{3.36}$$

Now we can write the sum over S_2 as:

$$L \left[\frac{f(\lambda_1, -\lambda_1)}{i(\lambda_1 + sk)} + \frac{f(-\lambda_1, \lambda_1)}{i(-\lambda_1 + sk)} \right]$$

$$- \frac{(a_2-1)f(\lambda_1,-\lambda_1)}{(\lambda_1+sk)^2} - \frac{(a_1-1)f(-\lambda_1,\lambda_1)}{(\lambda_1-sk)^2}. \quad (3.37)$$

and using equation (3.32) this becomes:

$$L\left[\frac{f(\lambda_1,-\lambda_1)}{i(\lambda_1+sk)} + \frac{f(-\lambda_1,\lambda_1)}{i(-\lambda_1+sk)}\right] + \frac{f(\lambda_1,-\lambda_1)-f(-\lambda_1,\lambda_1)}{(\lambda_1+sk)^2} + \frac{f(-\lambda_1,\lambda_1)-f(\lambda_1,-\lambda_1)}{(\lambda_1-sk)^2}. \quad (3.38)$$

Now we sum over $s = \pm 1$ to get:

$$L\left[\frac{f(\lambda_1,-\lambda_1)}{i(\lambda_1+k)} + \frac{f(-\lambda_1,\lambda_1)}{i(-\lambda_1+k)} + \frac{f(\lambda_1,-\lambda_1)}{i(\lambda_1-k)} + \frac{f(-\lambda_1,\lambda_1)}{i(-\lambda_1-k)}\right] \quad (3.39)$$

(all other terms cancel out in the s sum).

$$= L\left[\frac{f(\lambda_1,-\lambda_1)-f(-\lambda_1,\lambda_1)}{i(\lambda_1+k)} + \frac{f(\lambda_1,-\lambda_1)-f(-\lambda_1,\lambda_1)}{i(\lambda_1-k)}\right] \quad (3.40)$$

$$= -iL\left[f(\lambda_1,-\lambda_1)-f(-\lambda_1,\lambda_1)\right]\left[\frac{1}{\lambda_1+k}+\frac{1}{\lambda_1-k}\right]. \quad (3.41)$$

Now;

$$f(\lambda_1,-\lambda_1)-f(-\lambda_1,\lambda_1) = \frac{2\lambda_1+ic}{2\lambda_1} + \frac{2\lambda_1-ic}{2\lambda_1} = \frac{ic}{\lambda_1},$$

and:

$$\frac{1}{\lambda_1+k}+\frac{1}{\lambda_1-k} = \frac{\lambda_1-k+\lambda_1+k}{\lambda_1^2-k^2} = \frac{2\lambda_1}{\lambda_1^2-k^2}.$$

So equation (3.41) becomes:

$$\frac{2cL}{\lambda_1^2-k^2}, \quad (3.42)$$

and using equation (3.21) we get that the overlap of our initial state $|\psi\rangle$ with the unnormalized Bethe state $|\lambda_1,\lambda_2\rangle$ is:

$$\langle\psi|\lambda_1,-\lambda_1\rangle = \frac{2L}{C_N^\psi}\frac{\sqrt{2}c^2}{\lambda_1^2-k^2}. \quad (3.43)$$

3.4 General Overlap Method ($N \geq 2$) for Counter-Rotating BECs

We use a method outlined in [33, 34] in order to calculate the overlap. The overlap of one of our rotating BECs $|\psi\rangle$ with an arbitrary Bethe state $|\boldsymbol{\lambda_N}\rangle$ has the form:

$$\frac{\sqrt{c^N N!}}{C_N^\psi} \sum_{\substack{\sigma \in S_N \\ \mathbf{s} \in \mathrm{Sgn}_N^\psi}} \left[\prod_{j<l} f(\lambda_{\sigma_j}, \lambda_{\sigma_l}) \right] \times \int_{\mathbf{1}} \mathrm{d}x_N ... \mathrm{d}x_1 \exp\left[i \sum_j s_j k x_j \right] \exp\left[i \sum_{k=1}^N \lambda_{\sigma_k} x_k \right] \quad (3.44)$$

$$= \frac{\sqrt{c^N N!}}{C_N^\psi} \mathcal{S}_N^\psi(\{\lambda_{\mathbf{N}}\}, k), \quad (3.45)$$

where $\mathbf{1}$ is now the simplex given by $0 < x_1 < x_2 ... < x_N < L$. We must evaluate integrals of the following form:

$$\sum_{\mathbf{s} \in \mathrm{Sgn}_N^\psi} \int_{\mathbf{1}} \mathrm{d}x_N ... \mathrm{d}x_1 \exp\left(i \sum_j s_j k x_j \right) \exp\left[i \sum_{k=1}^N \lambda_k x_k \right]. \quad (3.46)$$

Recall the definition of $B_N(\alpha_1, ..., \alpha_N)$ from equation (3.22). We can then write equation (3.46) as

$$\mathcal{B}_N^\psi(\boldsymbol{\lambda}, k) := \sum_{s \in \mathrm{Sgn}_N^\psi} B_N(\boldsymbol{\lambda} + k\boldsymbol{s}). \quad (3.47)$$

While on the topic of the B function, I will quickly mention a result that can be found in [33] and will be relevant very soon:

$$B_N(\alpha_1, ..., \alpha_N) = \sum_{j=0}^N B_{N,j}(\alpha_1, ..., \alpha_N), \quad (3.48)$$

where

$$B_{N,j}(\alpha_1,...,\alpha_N) = (-1)^j \frac{\prod_{k=j+1}^{N} e^{i\alpha_k L}}{\left[\prod_{k=j+1}^{N}\sum_{m=j+1}^{k} i\alpha\right]\left[\prod_{k=1}^{j}\sum_{m=k}^{j} i\alpha\right]}. \quad (3.49)$$

and we define $\mathcal{B}^{\psi}_{N,j}$ by just summing the $B_{N,j}$ terms over Sgn^{ψ}_{N}

We know from the $N = 2$ case and [34] that we are looking only for the singular parts of this expression from taking the parity limit, ie, we are looking for the singular part of:

$$\mathcal{S}^{\psi}_{N}(\{\lambda_{\mathbf{N}}\},k) = \sum_{\sigma\in S_N}\left[\prod_{j<l} f(\lambda_{\sigma(j)},\lambda_{\sigma(l)})\right]\mathcal{B}^{\psi}_{N}(\sigma\boldsymbol{\lambda},k). \quad (3.50)$$

Let's start with finding the singular parts of $\mathcal{B}^{\psi}_{N}(\boldsymbol{\lambda},k)$. The singularity at the pole $\lambda_m{=}{-}\lambda_{m+1}$ can be found easily as described in [33]:

$$\begin{aligned}\mathrm{Res}_{\lambda_{m+1}\to-\lambda_m}\mathcal{B}^{\psi}_{N}(\boldsymbol{\lambda},k) \sim u^{\psi}_{N/2}\frac{a_m a_{m+1}-1}{i(\lambda_m+\lambda_{m+1})}\left(\frac{1}{i(\lambda_m+k)}+\frac{1}{i(\lambda_m-k)}\right)\\ \times\mathcal{B}^{\psi}_{N-2,m-1}(\{\lambda_j|,j\in\{1,...\cancel{m},\cancel{m+1},...,N\}\},k) \quad (3.51)\end{aligned}$$

$$\begin{aligned}= u^{\psi}_{N/2}\frac{a_m a_{m+1}-1}{i(\lambda_m+\lambda_{m+1})}\frac{2\lambda_m}{i(\lambda_m^2-k^2)}\\ \times\mathcal{B}_{\psi,N-2,m-1}(\{\lambda_j\},k\},j\in\{1,...\cancel{m},\cancel{m+1},...,N\}), \quad (3.52)\end{aligned}$$

where the strike through the m and $m+1$ indicates that we evaluate $\mathcal{B}$ for $N-2$ rapidities (excluding rapidities m and $m+1$). Here, u^{ψ}_{n} is a factor that counts the number of pairs of terms in $\mathcal{B}^{\psi}_{2n}$ that satisfy $s_p = -s_{p+1}$ when there are n pairs of rapidities left and just before rapidities p and $p+1$ are 'removed' (removed here means after calculating the corresponding residue). The pair being removed gives us the $2\lambda_p/(i(\lambda_p^2-k^2))$ term. We then sum over all permutations that have particles m and $m+1$ in neighbouring positions [34] and find the residue of $\mathcal{S}^{\psi}_{N}$ at $\lambda_m+\lambda_{m+1}=0$ is:

$$\mathcal{S}_N \sim u^{\psi}_{N/2} \frac{a_m a_{m+1} - 1}{i(\lambda_m + \lambda_{m+1})} F(\lambda_m) \times \prod_{j \neq m, m+1} f(\lambda_j, \lambda_1) f(\lambda_j, -\lambda_1) \mathcal{S}^{\psi,\mathrm{mod(m)}}_{N-2}(\cancel{m}, \cancel{m+1}), \quad (3.53)$$

where $\mathcal{S}^{\psi,\mathrm{mod(m)}}_{N-2}(\cancel{m}, \cancel{m+1})$ is $\mathcal{S}^{\psi}_N$ evaluated for $N-2$ rapidities (excluding rapidities m and $m+1$), and is evaluated with the modified a's instead of the normal a's (the modification depends on m):

$$a_j^{\mathrm{mod(m)}} = \frac{f(\lambda_m, \lambda_j)}{f(\lambda_j, \lambda_m)} \frac{f(\lambda_m, \lambda_j)}{f(\lambda_j, \lambda_m)} a_j \quad (3.54)$$

and the function $F(\lambda)$ is given by:

$$\begin{aligned} F(\lambda) &= \frac{f(\lambda, -\lambda)}{i(\lambda + k)} + \frac{f(\lambda, -\lambda)}{i(\lambda - k)} + \frac{f(-\lambda, \lambda)}{i(-\lambda + k)} + \frac{f(-\lambda, \lambda)}{i(-\lambda - k)} \\ &= \frac{2\lambda}{i(\lambda^2 - k^2)} f(\lambda, -\lambda) + \frac{-2\lambda}{i(\lambda^2 - k^2)} f(-\lambda, \lambda) \\ &= \frac{2c}{\lambda^2 - k^2}. \end{aligned} \quad (3.55)$$

3.4.1 Taking the Parity Limit

To calculate the exact on-shell overlap of the initial state with parity-symmetric Bethe States, we must perform the following [34] limiting procedure:

$$\lambda_{2j-1} \to \lambda_j^+, \quad \lambda_{2j} \to -\lambda_j^+, \quad j = 1, ..., N/2. \quad (3.56)$$

We then define the following variables for $j = 1, ..., N/2$:

$$m_j^+ = m(\lambda_j^+) = -i \frac{d}{d\lambda} \log(a(\lambda)) \Big|_{\lambda = \lambda_j^+}. \quad (3.57)$$

It can be easily checked that after taking the parity limit, we get that:

$$\frac{a_{2j-1} a_{2j} - 1}{i(\lambda_{2j-1} + \lambda_{2j})} \longrightarrow m_j^+. \quad (3.58)$$

Next, define the function $D_N^{\psi}(\boldsymbol{\lambda}_{N/2}^+, \boldsymbol{m}_{N/2}^+)$ to be the overlap $S_N^{\psi}(\boldsymbol{\lambda}_N; \boldsymbol{a}_N)$ after the full parity limit as described in equation (3.56) is taken. Then, using equation (3.53), it is easy to show that $D_N^{\psi}(\boldsymbol{\lambda}_{N/2}^+, \boldsymbol{m}_{N/2}^+)$ satisfies the recursion relation:

$$\frac{\partial D_N^{\psi}(\boldsymbol{\lambda}_{N/2}^+, \boldsymbol{m}_{N/2}^+)}{\partial m_j^+} = u_{N/2}^{\psi} F(\lambda_j^+) \prod_{k=1, k\neq j}^{N/2} \overline{f}(\lambda_k^+, \lambda_j^+) D_N^{\psi}(\boldsymbol{\lambda}_{N/2-1}^+, \boldsymbol{m}_{N/2-1}^{+,\mathrm{mod(j)}}), \tag{3.59}$$

where the modified m variables are defined as one would expect:

$$m^{\mathrm{mod(j)}}(\lambda_k^+) = -i\frac{d}{d\lambda} \log\big(a^{\mathrm{mod(j)}}(\lambda)\big)\Big|_{\lambda=\lambda_k^+} = m_k^+ + \varphi^+(\lambda_k^+, \lambda_j^+), \tag{3.60}$$

and $D_N^{\psi}(\boldsymbol{\lambda}_{N/2-1}^+, \boldsymbol{m}_{N/2-1}^+)$ is understood to have its j'th variables removed from its arguments. Using [34], the solution to the recursion relation equation (3.59) is:

$$D_N^{\psi}(\boldsymbol{\lambda}_{N/2}^+, \boldsymbol{m}_{N/2}^+) = U_N^{\psi} \prod_{j=1}^{N/2} F(\lambda_j^+) \prod_{1\leq k<j\leq N/2} \overline{f}(\lambda_k^+, \lambda_j^+) \det G^+, \tag{3.61}$$

where $U_N^{\psi} = \prod_{j=1}^{N/2} u_j^{\psi}$. Using equation (3.18) I then calculate the exact overlap of the given initial BEC state with the on-shell parity symmetric normalized Bethe state as:

$$U_N^{\psi} \frac{\sqrt{N!}}{C_N^{\psi}} \prod_{j=1}^{N/2} \frac{F(\lambda_j^+)}{\sqrt{f(\lambda_j^+, -\lambda_j^+) f(-\lambda_j^+, \lambda_j^+)}} \sqrt{\frac{\det G^+}{\det G^-}}$$

$$= U_N^{\psi} \frac{\sqrt{N!}/(c^N C_N^{\psi})}{\prod_{j=1}^{N/2} \frac{\lambda_j^{+2} - k^2}{2c\lambda_j^+} \sqrt{\frac{\lambda_j^{+2}}{c^2} + \frac{1}{4}}} \sqrt{\frac{\det G^+}{\det G^-}}$$

$$= U_N^{\psi} \frac{\sqrt{N! 2^N}/C_N^{\psi}}{\prod_{j=1}^{N/2} \frac{\lambda_j^{+2}-k^2}{\lambda_j^+} \sqrt{\frac{\lambda_j^{+2}}{c^2}+\frac{1}{4}}} \sqrt{\frac{\det G^+}{\det G^-}}. \tag{3.62}$$

Next, to find the overlaps for the specific initial states introduced at the start of this write up, we now need to calculate U_N^{ψ} for out different initial states. Recall the first initial state introduced, the 'Counter-Rotating BEC':

$$\langle \boldsymbol{x} | \psi_1 \rangle \sim \prod_{i=1}^{N} \left(e^{ikx_i} + e^{-ikx_i} \right). \tag{3.63}$$

To calculate U_N for this state, we must calculate the individual u_j's.

Let's go back to the recursion relation in equation (3.52) and let's first take there to be j pairs left. For ease of notation, we shall label the next pair of momenta we are calculating the residue in the parity limit of as λ_1 and λ_2.

We look to count the number of pairs of terms in $(e^{ikx_1} + e^{-ikx_1})(e^{ikx_2} + e^{-ikx_2})$, such that we have an equal number of $+k$ and $-k$ momenta in the each term of the pair. Multiplying this expression out, we see that we have one such pair, namely $e^{ikx_1 - ikx_2} + e^{-ikx_1 + ikx_2}$. So we get that u_j for this state is 1 for all j.

We now carry out the same calculation for the second initial state, the 'Fragmented BEC'. We carry out the same calculation as before except now we are looking at the sum $\sum_{\sigma \in S_{2j}} \exp\left[ik_{\sigma_1}x_1 + ik_{\sigma_2}x_2\right]$, where $\boldsymbol{k} = \{+k, -k, ..., +k, -k\}$ (vector of size 2j). There are j choices to make k_{σ_1} positive, and j choices to make k_{σ_2} negative, so we have a factor of j^2. We then have another j^2 choices for the signs being flipped, but we are counting the pairs of such terms with the signs flipped between them, so we get that $u_j = j^2$ for this state. To then calculate U_N for this state, we just note that;

$$U_N = \prod_{j=1}^{N/2} u_j = \prod_{j=1}^{N/2} j^2 = [(N/2)!]^2. \tag{3.64}$$

We then conclude this calculation by explicitly writing out the full overlaps

for our two initial states:

$$\langle\psi_1|\boldsymbol{\lambda}_N\rangle = \frac{(N!/L^N)^{1/2}}{\prod_{j=1}^{N/2}\frac{\lambda_j^{+2}-k^2}{\lambda_j^+}\sqrt{\frac{\lambda_j^{+2}}{c^2}+\frac{1}{4}}}\sqrt{\frac{\det G^+}{\det G^-}}, \tag{3.65}$$

$$\langle\psi_2|\boldsymbol{\lambda}_N\rangle = \frac{(N/2)!(2/L)^{N/2}}{\prod_{j=1}^{N/2}\frac{\lambda_j^{+2}-k^2}{\lambda_j^+}\sqrt{\frac{\lambda_j^{+2}}{c^2}+\frac{1}{4}}}\sqrt{\frac{\det G^+}{\det G^-}}. \tag{3.66}$$

3.4.2 Difference in Overlaps of the Two Initial States

The results we just found tell us something interesting: Looking at the above overlaps, it should be easy to see that if we project our initial states onto the subspace generated by parity symmetric Bethe states and re-normalise them, then the overlaps are the exact same across both initial states. Where the overlaps differ is only outside of this subspace. We can explicitly show that these two initial states have different overlaps outside of the parity symmetric subspace. I do this by looking how the conserved charges Q_j $(j = 1, 2, ...)$ of the Lieb–Liniger Hamiltonian act on our initial states. Writing down Q_j's action on states in position representation is difficult for general j, but I need only use Q_1 to illustrate my point, and its position representation is quite simple:

$$Q_1 = P = -i\sum_{j=1}^{N}\frac{\partial}{\partial x_j}. \tag{3.67}$$

Let's first look at the action of Q_1 on $\psi_1(\boldsymbol{x}) = \langle\boldsymbol{x}|\psi_1\rangle$:

$$\begin{aligned} Q_1\psi_1(\boldsymbol{x}) &= -i\left(\sum_{j=1}^{N}\frac{\partial}{\partial x_j}\right)\prod_{k=1}^{N}(e^{ikx_k}+e^{-ikx_k}) \\ &= k\sum_{j=1}^{N}\left[(e^{ikx_1}+e^{-ikx_k})...(e^{ikx_j}-e^{-ikx_k})...(e^{ikx_N}+e^{-ikx_N})\right] \\ &= ik2^N\left[\prod_{j=1}^{N}\cos(kx_j)\right]\left[\sum_{l=1}^{N}\tan(kx_l)\right], \end{aligned} \tag{3.68}$$

which is clearly not identically zero. Now let's have a look at the action of Q_1 on $\psi_2(\boldsymbol{x}) = \langle \boldsymbol{x}|\psi_2\rangle$:

$$\begin{aligned} Q_1\psi_2(\boldsymbol{x}) &= -i\left(\sum_{j=1}^{N}\frac{\partial}{\partial x_j}\right)\sum_{\sigma\in S_N} e^{i\sigma\boldsymbol{k}\cdot\boldsymbol{x}} \\ &= \sum_{j=1}^{N}\sum_{\sigma\in S_N} k_{\sigma_j} e^{i\sigma\boldsymbol{k}\cdot\boldsymbol{x}} \\ &= \sum_{\sigma\in S_N}\left(e^{i\sigma\boldsymbol{k}\cdot\boldsymbol{x}}\sum_{j=1}^{N} k_{\sigma_j}\right), \end{aligned} \tag{3.69}$$

which is identically zero since $\sum_{j=1}^{N} k_{\sigma_j} = 0$ for all $\sigma \in S_N$, where $\boldsymbol{k} = \{+k, -k, ..., +k, -k\}$. Specifically, if $N = 2$, then as we can see from the discussion above, $\psi_2(\boldsymbol{x})$ is an integrable state as all the odd conserved charges up to $N = 2$ annihilate it. This turns out to be the only (even) value for N in which $\psi_2(\boldsymbol{x})$ is integrable, as Q_3 does not annihilate it when $N = 4$. Moreover, as seen above, Q_1 does not annihilate $\psi_1(\boldsymbol{x})$ even when $N = 2$, so this state is not integrable for any (even) N.

3.5 Conclusion

In this chapter, I have presented a method to calculate the overlaps of parity symmetric Bethe states in the Lieb–Liniger model with a 'generic' initial state (provided you have the plane wave expansion of the initial state). I demonstrated this concretely using a counter-rotating BEC, and a fragmented BEC. The actual choice of the initial state was delayed until the very end of the calculation, showing the method's potential for generalisation to more initial states. Overlaps for quench-based calculations are generally quite hard to come across, so the more general a calculation is with respect to 'generic' initial states, the better. In the end, the main idea came down to just counting specific parity-symmetric pairs of plane waves in the initial state.

Following on from this, I then showed that the two initial states only differ in the non-parity symmetric region of the Hilbert space. In other words, if

we project both states onto the subspace spanned by the parity symmetric initial states and re-normalize them, we get the same state. As a result, I would expect $|\psi_1\rangle$ and $|\psi_2\rangle$ to have significant long time correlations [35], although maybe this is not overly clear.

Chapter 4

Entanglement Entropy in the Lieb–Liniger Model

In this chapter, I will present a method (of exponential computational complexity) for the analytic calculation of the spatial von Neumann bipartite entanglement entropy of energy eigenstates of the periodic Lieb–Liniger model. Numerical methods to calculate this object exist [12, 13] but to the best of my knowledge, this is the first analytic method. The only entropic object I will be interested in throughout this chapter is the von Neumann bipartite entanglement entropy, so it suffices to refer to this object as just the 'entanglement entropy' going forward.

I first introduce more clearly what I am calculating and give some motivations. Like the previous chapter, I then proceed with the calculation for the 2-particle case. This is then used to guide the calculation for the general N-particle case. Some numerical results for the 2-particle case are also provided in order to see if my results match up with what is expected.

4.1 Introduction to Entanglement Entropy

The von Neumann entropy of a state defined by the density matrix ρ is given by $-\operatorname{Tr}(\rho \log \rho)$ [36]. If we spatially partition our periodic Lieb–Liniger model into two parts A and B, we can then discuss the 'bipartite entanglement

entropy' between A and B. We partition the model by splitting our circle $[0, L)$ into two arcs $A = [0, l)$ and $B = [l, L)$.

If we are given the density matrix of some Bethe state $\rho^{AB} = |\psi\rangle\langle\psi|$, we can construct the reduced density matrix $\rho^A = \mathrm{Tr}_B\, \rho^{AB}$ by tracing only over the B 'part'. The entanglement entropy is then given by $-\mathrm{Tr}\big(\rho^A \log \rho^A\big)$ [11].

Using the Bethe Ansatz, we can write a generalised Bethe state as

$$|\psi(\boldsymbol{k})\rangle = \int_{\mathbf{1}} F(\boldsymbol{x}, \boldsymbol{k}) \prod_j \mathrm{d}x_j b^\dagger(x_j)\, |0\rangle\,, \tag{4.1}$$

where the domain $\mathbf{1}$ is given by $\{0 \leq x_1 < x_2 \leq L\}$. We need only integrate over $\mathbf{1}$ instead of the full $S^1 \times S^1$ due to symmetry of the system. The only thing that needs to be adjusted as a result is a factor of $N!$ in the normalisation of $|\psi\rangle$. The Bethe wavefunction $F(\boldsymbol{x}, \boldsymbol{k})$ is given by

$$F(\boldsymbol{x}, \boldsymbol{k}) = e^{ik_1x_1 + ik_2x_2} + S_{12} e^{ik_2x_1 + ik_1x_2}, \tag{4.2}$$

where

$$S_{12} = \frac{k_1 - k_2 + ic}{k_1 - k_2 - ic}. \tag{4.3}$$

All of the details for these calculations can be found in section (1.2.3).

4.2 Calculating an Expression for the Entanglement–Entropy in the 2 Particle Case

Let $\mathbf{1}_A$ and $\mathbf{1}_B$ represent the intersections of $\mathbf{1}$ with A^2 and B^2 respectively. The entanglement entropy of $|\psi\rangle$ is given by

$$-\mathrm{Tr}\big(\rho^A \log \rho^A\big), \tag{4.4}$$

where

$$\rho^A = \mathrm{Tr}_B\, \rho^{AB}, \tag{4.5}$$

and

$$\rho^{AB} = |\psi(\boldsymbol{k})\rangle \langle\psi(\boldsymbol{k})| = \int_{\mathbf{1}}\int_{\mathbf{1}} \mathrm{d}\boldsymbol{x}\mathrm{d}\boldsymbol{x}' F(\boldsymbol{x},\boldsymbol{k})F(\boldsymbol{x}',\boldsymbol{k}) |\boldsymbol{x}\rangle \langle\boldsymbol{x}'| . \tag{4.6}$$

Here I use $|\boldsymbol{x}\rangle$ to mean $b^\dagger(x_2)b^\dagger(x_1)|0\rangle$.

From now on, since I am looking at the entanglement entropy of a specific eigenstate, I will suppress the k–dependence in F.

Noting that $\mathrm{Tr}_B |x\rangle\langle x'| = \langle x'|x\rangle$ iff $x \in B$, we can write the reduced density matrix ρ^A for the system as:

$$\rho^A = \rho_0 + \rho_1 + \rho_2, \tag{4.7}$$

where:

$$\rho_0 = \int_{\boldsymbol{x}\in\mathbf{1}_B} \mathrm{d}\boldsymbol{x}|F(\boldsymbol{x})|^2 |0\rangle\langle 0| , \tag{4.8}$$

$$\rho_1 = \int_{x_1,x_1'\in A} \mathrm{d}x_1\mathrm{d}x_1' \int_{x_2\in B} \mathrm{d}x_2 F(x_1,x_2)F^*(x_1',x_2) |x_1\rangle\langle x_1'| , \tag{4.9}$$

and

$$\rho_2 = \int_{\boldsymbol{x},\boldsymbol{x}'\in\mathbf{1}_A} \mathrm{d}\boldsymbol{x}\mathrm{d}\boldsymbol{x}' F(\boldsymbol{x})F^*(\boldsymbol{x}') |\boldsymbol{x}\rangle\langle\boldsymbol{x}'| . \tag{4.10}$$

Since each ρ_i acts on and into subspaces with different particle numbers, we can write:

$$-\mathrm{Tr}\big(\rho^A \log\rho^A\big) = -\sum_i \mathrm{Tr}(\rho_i \log\rho_i). \tag{4.11}$$

In the coming calculations, I will drop the integration measures as the notation becomes cumbersome and difficult to read through. In places where the measures are dropped, everything should be obvious from the domain of integration.

We start by calculating $\mathrm{Tr}(\rho_0 \log\rho_0)$:

$$\rho_0 = \int_{\mathbf{1}_B} |F(\boldsymbol{x})|^2 |0\rangle\langle 0| \tag{4.12}$$

$$\implies \log(\rho_0) = \log\left(\int_{\mathbf{1}_B} |F(\boldsymbol{x})|^2\right) |0\rangle\langle 0| \tag{4.13}$$

$$\implies \rho_0 \log(\rho_0) = \beta \log(\beta) |0\rangle\langle 0|, \tag{4.14}$$

where $\beta = \int_{\mathbf{1}_B} |F(\boldsymbol{x})|^2$.

$$\implies \mathrm{Tr}(\rho_0 \log \rho_0) = \beta \log(\beta). \tag{4.15}$$

Moving on, we next calculate $\mathrm{Tr}(\rho_2 \log \rho_2)$:

$$\rho_2 = \int_{\mathbf{1}_A^2} F(\boldsymbol{x})F^*(\boldsymbol{x}') |\boldsymbol{x}\rangle\langle\boldsymbol{x}'| \tag{4.16}$$

$$\begin{aligned}\implies \rho_2^2 &= \int_{\mathbf{1}_A^4} F(\boldsymbol{x})F^*(\boldsymbol{x}')F(\boldsymbol{y})F^*(\boldsymbol{y}') |\boldsymbol{x}\rangle\langle\boldsymbol{x}'|\boldsymbol{y}\rangle\langle\boldsymbol{y}'| \\ &= \int_{\mathbf{1}_A^3} F(\boldsymbol{x})F^*(\boldsymbol{x}')F(\boldsymbol{x}')F^*(\boldsymbol{y}') |\boldsymbol{x}\rangle\langle\boldsymbol{y}'| \\ &= \int_{\mathbf{1}_A^3} |F(\boldsymbol{x}')|^2 F(\boldsymbol{x})F^*(\boldsymbol{y}') |\boldsymbol{x}\rangle\langle\boldsymbol{y}'| \\ &= \left[\int_{\mathbf{1}_A} |F(\boldsymbol{x}')|^2\right] \rho_2. \end{aligned} \tag{4.17}$$

By induction, it is easy to see that:

$$\rho_2^n = \alpha^{n-1}\rho_2, \tag{4.18}$$

where $\alpha = \int_{\boldsymbol{x}\in\mathbf{1}_A} |F(\boldsymbol{x})|^2$. We can use this to calculate $\rho_2 \log \rho_2$:

$$\log(\rho_2) = \sum_{n=1}^{\infty} \frac{(-1)^{n+1}}{k} (\rho_2 - \mathbb{1})^n. \tag{4.19}$$

We expand the bracket above:

$$\begin{aligned}&(-\mathbb{1} + \rho_2)^n \\ &\quad = (-1)^n \mathbb{1} + \left[n(-1)^{n-1} + \binom{n}{2}(-1)^{n-2}\alpha + \binom{n}{3}(-1)^{n-3}\alpha^2 + ...\right] \rho_2\end{aligned}$$

$$= (-1)^n \mathbb{1} + \frac{(-1)^n[(1-\alpha)^n - 1]}{\alpha}\rho_2 = (-1)^n \left[\mathbb{1} + \frac{(1-\alpha)^{n-1}}{\alpha}\rho_2\right], \quad (4.20)$$

and so $\log \rho_2$ becomes:

$$\log(\rho_2) = -\sum_{n=1}^{\infty} \frac{1}{n}\left[\mathbb{1} + \frac{(1-\alpha)^{n-1}}{\alpha}\rho_2\right] \quad (4.21)$$

$$\implies \rho_2 \log \rho_2 = -\sum_{n=1}^{\infty} \frac{1}{n}\left[\rho_2 + \frac{(1-\alpha)^{n-1}}{\alpha}\rho_2^2\right]$$

$$= -\sum_{n=1}^{\infty} \frac{1}{n}\left[\rho_2 + (1-\alpha)^{n-1}\rho_2\right] = -\rho_2 \sum_{n=1}^{\infty} \frac{(1-\alpha)^n}{n} = \rho_2 \log(\alpha) \quad (4.22)$$

$$\implies \mathrm{Tr}(\rho_2 \log \rho_2) = (\log \alpha)\,\mathrm{Tr}\,\rho_2 = \alpha \log \alpha. \quad (4.23)$$

Lastly, we must calculate $\mathrm{Tr}(\rho_1 \log \rho_1)$ which is by far the most involved part of this calculation.

$$\rho_1 = \int_{A^2} \mathrm{d}x_1 \mathrm{d}x_1' \int_B \mathrm{d}x_2 F(x_1, x_2) F^*(x_1', x_2) \left|x_1\right\rangle \left\langle x_1'\right|. \quad (4.24)$$

If we define the function

$$G(x, y) := \int_B F(x, z) F^*(y, z) \mathrm{d}z, \quad (4.25)$$

we can then write ρ_1 as:

$$\rho_1 = \int_{A^2} G(x, y) \left|x\right\rangle \left\langle y\right|. \quad (4.26)$$

Note that:

$$\rho_1^2 = \int_{A^4} G(x, y) G(z, w) \left|x\right\rangle \left\langle y|z\right\rangle \left\langle w\right|$$

$$= \int_{A^3} G(x, y) G(y, w) \left|x\right\rangle \left\langle w\right|$$

$$= \int_{A^2} [\mathcal{L}(G)](x,w) \left|x\right\rangle \left\langle w\right| , \tag{4.27}$$

where $\mathcal{L}$ is the integral operator with kernel G given by:

$$[\mathcal{L}(f)](x,w) = \int_A f(x,y)G(y,w)\mathrm{d}y. \tag{4.28}$$

Note that $G(x,y)^* = G(y,x)$ and so $\mathcal{L}$ is a self-adjoint operator. Also from the defintion of G in terms of the Bethe wavefunction F, it is easy to see that $\mathcal{L}$ is also a compact operator.

It can be shown by induction that:

$$\rho_1^n = \int_{A^2} \mathcal{L}^{n-1}(G) \left|x\right\rangle \left\langle w\right| . \tag{4.29}$$

We can then use this fact to calculate $\rho_1 \log \rho_1$:

$$\begin{aligned}
\log(\rho_1) &= \sum_{n=1}^{\infty} \frac{(-1)^{n+1}}{n} (\rho_1 - \mathbb{1})^n \\
&= \sum_{n=1}^{\infty} \frac{(-1)^{n+1}}{n} \sum_{j=0}^{n} \binom{n}{j} (-\rho_1)^j \qquad (4.30) \\
\implies \rho_1 \log \rho_1 &= \sum_{n=1}^{\infty} \frac{(-1)^{n+1}}{n} \sum_{j=0}^{n} \binom{n}{j} (-1)^j (\rho_1)^{j+1} \\
&= \sum_{n=1}^{\infty} \frac{(-1)^{n+1}}{n} \sum_{j=0}^{n} \binom{n}{j} (-1)^j \int_{A^2} \mathcal{L}^j(G) \left|x\right\rangle \left\langle w\right| \\
&= \sum_{n=1}^{\infty} \frac{(-1)^{n+1}}{n} \int_{A^2} \left[\sum_{j=0}^{n} \binom{n}{j} (-1)^j \mathcal{L}^j \right] (G) \left|x\right\rangle \left\langle w\right| \\
&= \sum_{n=1}^{\infty} \frac{(-1)^{n+1}}{n} \int_{A^2} [(\mathcal{L} - \mathbb{1})^n](G) \left|x\right\rangle \left\langle w\right| \\
&= \int_{A^2} \left[\sum_{n=1}^{\infty} \frac{(-1)^{n+1}}{n} (\mathcal{L} - \mathbb{1})^n \right] (G) \left|x\right\rangle \left\langle w\right| \\
&= \int_{A^2} [\log(\mathcal{L})](G) \left|x\right\rangle \left\langle w\right| \qquad (4.31)
\end{aligned}$$

$$\implies -\operatorname{Tr}\rho_1 \log \rho_1 = -\int_{A^2} [\log(\mathcal{L})](G)\delta(x-w). \tag{4.32}$$

Now we just need to investigate the operator $\log(\mathcal{L})$. In short, we notice that we can write $G(x,y) = \sum_{j=1}^{2} \phi_j(x)\chi_j(y)$ where each ϕ_j and χ_j $j = 1,2$ are continuous complex functions. Explicitly, we write the component functions in table(4.1).

Component Functions		
i	$\phi_i(x)$	$\chi_i(y)$
1	$e^{ik_1 x}$	$\phi_1^*(y)\left[\int_B \lvert\phi_2\rvert^2\right] + S_{12}^*\phi_2^*(y)\left[\int_B \phi_2\phi_1^*\right]$
2	$e^{ik_2 x}$	$S_{12}\phi_1^*(y)\left[\int_B \phi_1\phi_2^*\right] + \lvert S_{12}\rvert^2\phi_2^*(y)\left[\int_B \lvert\phi_1\rvert^2\right]$

Table 4.1: A table of component functions in the single variable decomposition of $G(x,y)$.

Note that $\mathcal{L}$ acts on $G(x,y)$ in the following way:

$$[\mathcal{L}(G)](x,w) = \sum_{j,k} \phi_j(x)\chi_k(w)\int_A \chi_j(y)\phi_k(y). \tag{4.33}$$

Back to the calculation at hand, using our ability to separate variables in G, we can write equation (4.32) as:

$$\begin{aligned} &-\sum_j \int_{A^2} \delta(x-w)\phi_j(x)[\log(\mathcal{L})](\chi_j)(w) \\ =&-\sum_j \int_A \phi_j(x)[\log(\mathcal{L})](\chi_j)(x), \end{aligned} \tag{4.34}$$

where

$$\mathcal{L}(\chi_j)(x) = \sum_k \chi_k(x)\int_A \chi_j(y)\phi_k(y), \tag{4.35}$$

so we only need to consider how $\mathcal{L}$ acts on functions of one variable. In this respect, $\mathcal{L}$ is a self-adjoint Hilbert-Schmidt integral operator. We thus proceed as follows in order to diagonalize $\mathcal{L}$.

1. f(x) is an eigenfunction of $\mathcal{L}$ with eigenvalue 0 iff $\langle f, \phi_j \rangle = 0$ for all ϕ_j.

2. $\lambda^l \neq 0$ is an eigenvalue of $\mathcal{L}$ iff $\det_{jk}(a_{jk} - \lambda^l \delta_{jk}) = 0$ where $a_{jk} = \int_A \phi_j(y)\chi_k(y)\mathrm{d}y$.

3. The corresponding eigenfunction $f^l(x)$ is given by $f^l(x) = \sum_j c_j^l \chi_j(x)$ where the c_j^l's are given by the following system of linear equations:

$$\sum_k (a_{jk} - \lambda^l \delta_{jk}) c_k^l = 0 \qquad \text{for all } j. \tag{4.36}$$

4. Using the fact that $f^l(x) = \sum_j c_j^l \chi_j(x)$, we get that $\chi_j(x) = \sum_l (c_j^l)^{-1} f^l(x)$ where the $(c_j^l)^{-1}$ are the coefficients of the inverse of the matrix (c_j^l).

Above I have used the fact that $\{\chi_j\}$ is a set of linearly independent functions. Note that they are only linearly dependant when $k_1 = k_2$, in which case $\chi_1 = \chi_2$ and so we are left with solving a one-dimensional system above.

Also, from point 1 above, we see that there are no eigenfunctions with eigenvalue 0 present in the decomposition of χ_j – which is what our operator is acting on. We can now calculate the action of $\log(\mathcal{L})$ on χ_j:

$$[\log(\mathcal{L})](\chi_j) = [\log(\mathcal{L})] \sum_l (c_j^l)^{-1} f^l \tag{4.37}$$

$$= \sum_l (c_j^l)^{-1} \log \lambda^l f^l. \tag{4.38}$$

Therefore, using equation (4.34) we get:

$$\begin{aligned} -\operatorname{Tr} \rho_1 \log \rho_1 &= -\sum_{j,l} (c_j^l)^{-1} \log \lambda^l \int_A \phi_j(x) f^l(x) \\ &= -\sum_{j,k,l} (c_j^l)^{-1} \log \lambda^l \int_A \phi_j(x) c_k^l \chi_k(x) \\ &= -\sum_{j,k,l} a_{jk} c_k^l \log \lambda^l (c_j^l)^{-1} \\ &= -\operatorname{Tr}\big(C A^T C^{-1} [\log \Lambda]\big), \end{aligned} \tag{4.39}$$

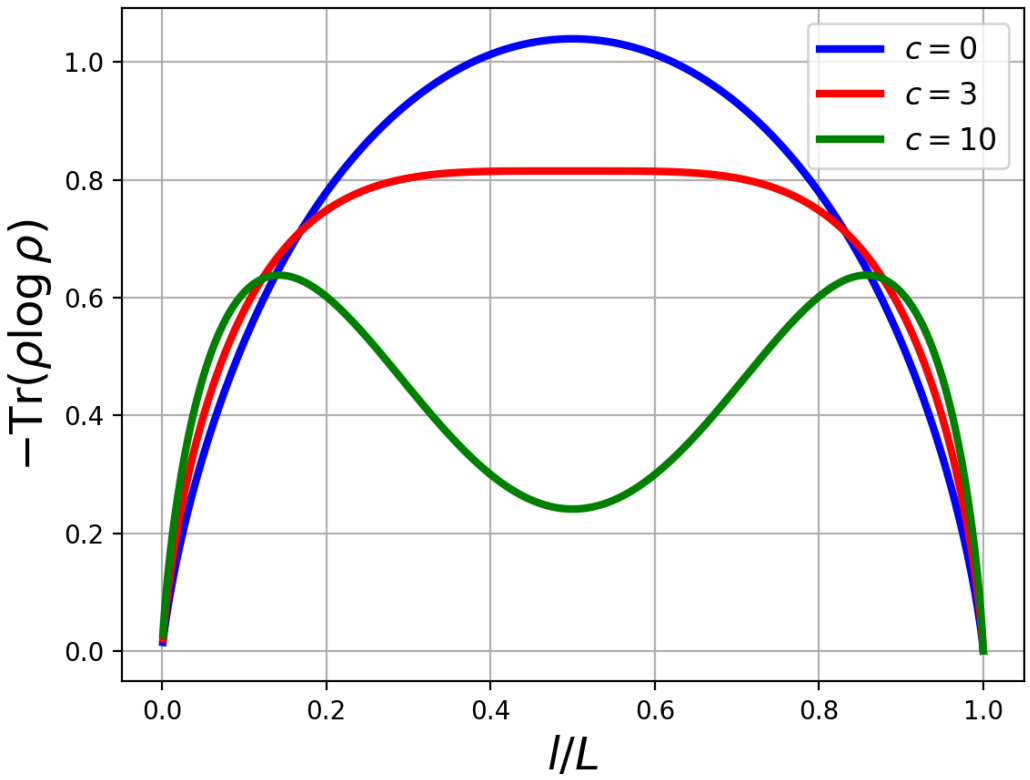

Figure 4.1: The von Neumann bipartite entanglement entropy of the ground state of our system, as a function of our subsystem fraction l/L with different values of c

where we define the matrices $A = (a_{jk})$, $C = (c_{jk})$, $\Lambda = \mathrm{diag}(\lambda_l)$. We can then write the full expression for the entanglement entropy as:

$$-\operatorname{Tr}\rho^A \log \rho^A = -\alpha \log \alpha - \beta \log \beta - \operatorname{Tr}\big(CA^T C^{-1}[\log \Lambda]\big). \tag{4.40}$$

In figure (4.2) I plot the above expression for various values of the interaction parameter c for the ground state as a function of the subsystem fraction l/L.

4.3 Generalization to the N-Particle Case

We proceed similarly to the 2-particle case. First we split the entanglement entropy into its different particle sectors as before:

$$\rho^A = \sum_j \rho_j, \tag{4.41}$$

where ρ_m represents the integral with m particles in subsystem A. Let $\boldsymbol{x} = (x_1, ..., x_m)$ be the coordinates for the particles in subsystem A, and $\boldsymbol{y} = (y_1, ..., y_{n-m})$ the coordinates for the particles in subsystem B. Similar to the 2-particle case, we define the simplex $\mathbf{1} = \{z \in \mathbb{R}^m | 0 \leq z_1 < z_2 < ... < z_m \leq L\}$ where the dimension of the simplex m is implied by the context of the relevant integral. We also define $\mathbf{1}_{A,B}$ to be the restrictions of the simplex $\mathbf{1}$ to A^m and B^m respectively. Now we can write:

$$\rho_m = \int_{\mathbf{1}_A^2} G_m(\boldsymbol{x}, \boldsymbol{x}') \left|\boldsymbol{x}\right\rangle \left\langle \boldsymbol{x}'\right|, \tag{4.42}$$

where

$$G_m(\boldsymbol{x}, \boldsymbol{x}') = \int_{\mathbf{1}_B} F(\boldsymbol{x}, \boldsymbol{y}) F^*(\boldsymbol{x}', \boldsymbol{y}) \mathrm{d}\boldsymbol{y}. \tag{4.43}$$

Then:

$$\rho_m^2 = \int_{\mathbf{1}_A^3} G_m(\boldsymbol{x}, \boldsymbol{x}') G_m(\boldsymbol{x}', \boldsymbol{x}'') \left|\boldsymbol{x}\right\rangle \left\langle \boldsymbol{x}''\right| = \int_{\mathbf{1}_A^2} [\mathcal{L}_m(G_m)](\boldsymbol{x}, \boldsymbol{x}'') \left|\boldsymbol{x}\right\rangle \left\langle \boldsymbol{x}''\right|, \tag{4.44}$$

where

$$[\mathcal{L}_m(f)](\boldsymbol{x}, \boldsymbol{x}'') = \int_{\mathbf{1}_A} f(\boldsymbol{x}, \boldsymbol{x}') G_m(\boldsymbol{x}', \boldsymbol{x}'') \mathrm{d}\boldsymbol{x}'. \tag{4.45}$$

It should be clear that we can always separate variables in $G_m(x, y)$, ie, there exist continuous complex functions ϕ_{m_j}, χ_{m_j}, $j = 1, ..., \binom{n}{m}$ such that $G_m(x, y) = \sum_j \phi_{m_j}(x) \chi_{m_j}(y)$. Proceeding like before, we arrive at:

$$-\operatorname{Tr}(\rho_m \log \rho_m) = -\sum_j \int_{\mathbf{1}_A} \phi_j(\boldsymbol{x}) [\log(\mathcal{L}_m)](\chi_{m_j}(\boldsymbol{x})). \tag{4.46}$$

We also again define the integrals:

$$a_{m_{jk}} = \int_{\mathbf{1}_A} \phi_{m_j}(\boldsymbol{x})\chi_{m_k}(\boldsymbol{x}). \tag{4.47}$$

We gather the eigenvalues λ^l like before, and define the matrices A_m, C_m and Λ_m similarly also, with subscripts to indicate which particle sector they belong to. We end up with the same expression as before:

$$-\operatorname{Tr}(\rho_m \log \rho_m) = -\operatorname{Tr}\big(C_m A_m^T C_m^{-1}[\log \Lambda_m]\big). \tag{4.48}$$

Using equation (4.41), we get our entanglement entropy:

$$-\operatorname{Tr}\big(\rho^A \log \rho^A\big) = -\sum_{m=0}^{N} -\operatorname{Tr}\big(C_m A_m^T C_m^{-1}[\log \Lambda_m]\big). \tag{4.49}$$

It is worth noting that just because we found the expression above, this does not mean that it is easy to calculate. Namely, if we have n bosons on our circle, we must calculate A_m, Λ_m, and C_m for each $0 \leq m \leq n$ (although the $m = 0$ and $m = n$ contributions can always be calculated using an easier method as in the $N = 2$ case in section (4.2)). We get A_m by calculating the $\left[\binom{n}{m}\right]^2$ integrals $a_{m_{jk}}$, we get Λ_m by diagonalizing the $\mathcal{L}_m$ operator, and we get C_m by solving the resulting systems of linear equations (see equation (4.36)).

Finally, we have a sum of $N+1$ similar looking terms in equation (4.49). This might lead one to believe that the result is somewhat proportional to N. Although we expect the entanglement entropy to indeed be $\mathcal{O}(N)$, this is not because of the above reason. Each of the individual terms should be expected to vary wildly in size. For example, if we have N large, we should expect large contributions from the terms around $m = N/2$, and then the rest to make negligible contributions.

4.4 Conclusion

In this chapter, I have presented a method for analytically calculating the spatial bipartite entanglement entropy of the Lieb–Liniger model. Although this method offers no speed up over numerical methods, the goal of finding an analytic expression for this object was to perhaps shed light on its mathematical structure. The existence of the method depends on being able to smoothly separate the variables in the function $G_m(\boldsymbol{x}, \boldsymbol{x}')$ from equation (4.43). This ability to smoothly separate variables in G comes from the nice plane wave packaging in which the Bethe wavefunction $F(\boldsymbol{x})$ comes to us in, and so this calculation method being a phenomenon of Bethe-solvable systems seems clear.

Furthermore, apart from this nice packaging I just mentioned, one might notice that the exact expression for $F(\boldsymbol{x})$ is not actually important in the outlined method for calculation. We should thus be able to generalise this method of calculating the bipartite entanglement entropy to any one-dimensional Bethe-solvable system in the continuum.

The next step from here would be to use the method above (with the help of some computer algebra/numerics) in order to calculate this entanglement entropy for various systems with larger numbers of particles. This would help confirm exactly how the spatial entanglement entropy of the eigenstates scale with system size.

Appendix A

Power Sum Proof

The purpose of this appendix is the prove the assertion equation (3.6) in section (3.2).
We set out to prove that given N even;

$$p_m(\boldsymbol{z}) = 0 \quad \forall\, m < N,\ m \text{ odd} \implies p_{m'}(\boldsymbol{z}) = 0 \quad \forall\, m' > N,\ m' \text{ odd},$$

where $\boldsymbol{z} = (z_1, z_2, ..., z_N)$ and $p_l(\boldsymbol{z}) = \sum_j z^l$.

Firstly, let's consider one of the Girard-Newton formulae [37]:

$$me_m + \sum_{j=1}^{m} (-1)^j e_{m-j} p_j = 0 \tag{A.1}$$

for $1 \leq m \leq N$, and where e_l and p_l are the l-th elementary polynomial and power sum for $\boldsymbol{z}$ respectively. I will show by induction that $p_m(\boldsymbol{z}) = 0 \quad \forall\, m < N,\ m \text{ odd} \implies e_m = 0$ for all m odd, $m < N$.

$\underline{m = 1}$:
For $m = 1$, equation (A.1) gives us:

$$e_1 = p_1,$$

and since p_1 is zero by assumption, e_1 is zero.

We now assume that e_m is zero for all odd m up to and including some

$s-2$ where $s < N$ odd.

Show for $m = s$:
Using equation (A.1) again, we get that:

$$se_s + \sum_{j=1}^{s} (-1)^j e_{s-j} p_j = 0. \tag{A.2}$$

Looking at the terms in the j sum, if j is odd, then we know from the starting assumption that $p_j = 0$. If instead j is even and $j \geq 2$, our induction hypothesis asserts that $e_{m-j} = 0$. This means we can write equation (A.2) as:

$$se_s = 0 \implies e_s = 0$$

proving our induction hypothesis.

Recall that we are here to show that $p_m = 0$ for all m odd, $m > N$. I now use another one of the Girard-Newton formulae [37]:

$$\sum_{j=m-N}^{m} (-1)^j e_{m-j} p_j = 0 \tag{A.3}$$

for $m > N$.

We now show that $p_m = 0$ for all m odd, $m > N$ via induction.

$m = N + 1$:
equation (A.3) becomes:

$$\sum_{j=1}^{N+1} (-1)^j e_{N+1-j} p_j = 0. \tag{A.4}$$

We focus on the individual terms in the j sum. If $j < N$ is odd, then $p_j = 0$ from our starting assumption. Note that given the limits of the sum, $1 \leq N + 1 - j \leq N$, so if j is instead even, then since $N + 1 - j$ is odd, from the previous inductive exercise we get that $e_{N+1-j} = 0$.

Using these results, we can rewrite equation (A.4) as:

$$p_{N+1} = 0,$$

proving our statement for $m = N + 1$.

We then assume the statement to be true for all m odd from $m = N + 1$ to $m = s - 2$ where s odd.

Show for $m = s$:
equation (A.3) becomes:

$$\sum_{j=s-N}^{s} (-1)^j e_{s-j} p_j = 0. \tag{A.5}$$

We focus on the individual terms of the j sum yet again. If $N + 1 < j < s$ odd, then from our inductive hypothesis, we get that $p_j = 0$. Note that given the limits of the sum, $0 \leq s - j \leq N$, so if j is instead even, then since $s - j$ is odd, from the previous inductive exercise we get that $e_{s-j} = 0$. Using these results, we can rewrite equation (A.5) as:

$$p_s = 0,$$

proving our inductive hypothesis.

Overall, this shows that given

$$p_m(\boldsymbol{z}) = 0 \quad \forall\, m < N,\ m \text{ odd},$$

we get that:

$$p_{m'}(\boldsymbol{z}) = 0 \quad \forall\, m' > N,\ m' \text{ odd},$$

proving our claim.

Bibliography

[1] R Toskovic, R van den Berg, A Spinelli, IS Eliens, B van den Toorn, B Bryant, J-S Caux, and AF Otte. Atomic spin-chain realization of a model for quantum criticality. *Nature Physics*, 12(7):656–660, 2016.

[2] M Ozerov, E Čižmár, J Wosnitza, SA Zvyagin, F Xiao, CP Landee, and MM Turnbull. Magnetic properties of the s= 1/2 heisenberg spin-chain material (6map) cucl3. In *Journal of Physics: Conference Series*, volume 150, page 042159. IOP Publishing, 2009.

[3] Jon Links, Katrina E Hibberd, et al. Bethe ansatz solutions of the bose-hubbard dimer. *SIGMA. Symmetry, Integrability and Geometry: Methods and Applications*, 2:095, 2006.

[4] Pedro S Goldbaum. Existence of solutions to the Bethe ansatz equations for the 1D Hubbard model: Finite lattice and thermodynamic limit. *Communications in mathematical physics*, 258(2):317–337, 2005.

[5] Fabian HL Essler, Holger Frahm, Frank Göhmann, Andreas Klümper, and Vladimir E Korepin. *The one-dimensional Hubbard model*. Cambridge University Press, 2005.

[6] Albert Einstein. Quantum theory of the monatomic ideal gas. *Sitzungsberichte der Preussischen Akademie der Wissenschaften, Physikalisch-mathematische Klasse*, pages 261–267, 1924.

[7] Michel Gaudin. *The Bethe Wavefunction*. Cambridge University Press, 2014.

[8] Nikita Andreevich Slavnov. Algebraic Bethe ansatz. *arXiv preprint arXiv:1804.07350*, 2018.

[9] Jacopo De Nardis, Bram Wouters, Michael Brockmann, and Jean-Sébastien Caux. Solution for an interaction quench in the Lieb–Liniger bose gas. *Physical Review A*, 89(3):033601, 2014.

[10] Lorenzo Piroli, Balázs Pozsgay, and Eric Vernier. What is an integrable quench? *Nuclear Physics B*, 925:362–402, 2017.

[11] Matthew Headrick. Lectures on entanglement entropy in field theory and holography. *arXiv preprint arXiv:1907.08126*, 2019.

[12] CM Herdman, P-N Roy, RG Melko, and A Del Maestro. Spatial entanglement entropy in the ground state of the Lieb–Liniger model. *Physical Review B*, 94(6):064524, 2016.

[13] Bernd Schmidt and Michael Fleischhauer. Exact numerical simulations of a one-dimensional trapped bose gas. *Physical Review A*, 75(2):021601, 2007.

[14] Hans Bethe. Zur Theorie der Metalle. *Zeitschrift für Physik*, 71(3-4):205–226, 1931.

[15] Fabio Franchini. Notes on Bethe ansatz techniques. *International School for Advanced Studies-Trieste, Lecture Notes*, 2011.

[16] Deok-Sun Lee and Doochul Kim. Bethe ansatz solutions and excitation gap of the attractive Bose–Hubbard model. *arXiv preprint cond-mat/0108314*, 2001.

[17] TC Choy and FDM Haldane. Failure of Bethe-ansatz solutions of generalisations of the Hubbard chain to arbitrary permutation symmetry. *Physics Letters A*, 90(1-2):83–84, 1982.

[18] Norman Oelkers and Jon Links. Ground-state properties of the attractive one-dimensional Bose–Hubbard model. *Physical Review B*, 75(11):115119, 2007.

[19] Fabian HL Eβler, Vladimir E Korepin, and Kareljan Schoutens. Completeness of the SO(4) extended Bethe ansatz for the one-dimensional Hubbard model. *Nuclear Physics B*, 384(3):431–458, 1992.

[20] Fabio Franchini. *An introduction to integrable techniques for one-dimensional quantum systems*. Springer, 2017.

[21] Vladimir E Korepin, Nicholay M Bogoliubov, and Anatoli G Izergin. *Quantum inverse scattering method and correlation functions*, volume 3. Cambridge university press, 1997.

[22] Oleg Derzhko. Jordan–Wigner fermionization and the theory of low-dimensional quantum spin models. Dynamic properties. In *Condensed Matter Physics in the Prime of the 21st Century: Phenomena, Materials, Ideas, Methods*, pages 35–87. World Scientific Publishing Company Incorporated, 2008.

[23] Michael Brockmann. Unpublished notes, 2018.

[24] Minoru Takahashi. One-dimensional Heisenberg model at finite temperature. *Progress of Theoretical Physics*, 46(2):401–415, 1971.

[25] Minoru Takahashi. *Thermodynamics of one-dimensional solvable models*. Cambridge university press, 2005.

[26] Michel Gaudin, Barry M McCoy, and Tai Tsun Wu. Normalization sum for the Bethe's hypothesis wave functions of the Heisenberg–Ising chain. *Physical Review D*, 23(2):417, 1981.

[27] Vladimir E Korepin. Calculation of norms of Bethe wave functions. *Communications in Mathematical Physics*, 86(3):391–418, 1982.

[28] Fabian HL Essler, Vladimir E Korepin, and Kareljan Schoutens. Fine structure of the Bethe ansatz for the spin-1/2 Heisenberg XXX model. *Journal of Physics A: Mathematical and General*, 25(15):4115, 1992.

[29] Rob Hagemans and Jean-Sébastien Caux. Deformed strings in the Heisenberg model. *Journal of Physics A: Mathematical and Theoretical*, 40(49):14605, 2007.

[30] Jean-Sébastien Caux. The quench action. *Journal of Statistical Mechanics: Theory and Experiment*, 2016(6):064006, 2016.

[31] Jean-Sébastien Caux and Fabian HL Essler. Time evolution of local observables after quenching to an integrable model. *Physical review letters*, 110(25):257203, 2013.

[32] Leda Bucciantini. Stationary state after a quench to the Lieb–Liniger from rotating BECs. *Journal of Statistical Physics*, 164(3):621–644, 2016.

[33] Hui-Huang Chen. Exact overlaps in the lieb-liniger model from coordinate bethe ansatz. *Physics Letters B*, 808:135631, 2020.

[34] Yunfeng Jiang and Balázs Pozsgay. On exact overlaps in integrable spin chains. *Journal of High Energy Physics*, 2020(2002.12065):1–35, 2020.

[35] Joshua M Deutsch. Eigenstate thermalization hypothesis. *Reports on Progress in Physics*, 81(8):082001, 2018.

[36] Dénes Petz. Entropy, von-Neumann and the von-Neumann entropy. In *John von Neumann and the foundations of quantum physics*, pages 83–96. Springer, 2001.

[37] DG Mead. Newton's identities. *The American mathematical monthly*, 99(8):749–751, 1992.